

Aus dem medizinischen Zentrum für Radiologie
Klinik für Strahlentherapie und Radioonkologie
Direktorin: Professor Dr. med. Rita Engenhardt-Cabillic

der Philipps-Universität Marburg
in Zusammenarbeit
mit dem Universitätsklinikum Gießen und Marburg GmbH,
Standort Marburg

Gene expression profiling of lung cancer cells irradiated by carbon ion and X-rays



Inaugural-Dissertation
zur Erlangung des Doktorgrades dem Fachbereich Pharmazie der
Phillips-Universität Marburg

vorgelegt von

An You
aus
VR. China
Marburg 2012

Angenommen vom Fachbereich Pharmazie der Philipps-Universität
Marburg am:

Gedruckt mit Genehmigung des Fachbereichs.

Dekan: Prof. Dr. M. Keusgen

Referent: Prof. Dr. M. Keusgen

Korreferent: Prof. Dr. R. Engenhardt-Cabillic

Table of Contents

1. Introduction	6
1.1. Conventional treatment for lung cancer.....	6
1.2. Charged particle beam radiation therapy.....	7
1.2.1. Charged particle radiation.....	7
1.2.2. Biophysical advantages of charged particle radiation.....	8
1.2.3. Charged particle irradiation applied in cancer therapy.....	11
1.2.4. Charged particle irradiation applied in NSCLC	11
1.3. Gene expression changes induced by irradiation.....	13
1.3.1. Gene expression changes induced by X-ray.....	14
1.3.2. Gene expression changes induced by heavy ion beams	15
1.4. Modern technologies applied in studying of gene functions.....	16
1.4.1. Microarray technology in biomedical and clinical research.....	17
1.4.2. Microarray technology applied in lung cancer research.....	18
1.4.3. Gene expression profiling using microarray technology in cancer research.....	19
1.5. The aim of this study	21
2. Materials	22
2.1. Cell line	22
2.2. Primers	22
2.3. Chemicals.....	23
2.4. Experiment Kits	24
2.5. Reagents.....	24
2.6. Consumable	24
2.7. Apparatus	24
2.8. Buffers and medium	25
3. Methods	27
3.1. Cell culture	27
3.1.1. Thawing cultured cells	27
3.1.2. Trypsinizing and subculturing cells.....	27
3.2. Radiation	27
3.3. Colony forming assay	29

3.4. Microarray analysis.....	29
3.4.1. RNA-extraction.....	29
3.4.2. Quantitative and qualitative analysis of RNA.....	30
3.4.3. RNA amplification.....	30
3.4.4. cDNA synthesis.....	30
3.4.5. cDNA labeling.....	31
3.4.6 Microarray experiments.....	31
3.5. Quantification of genes expression using qRT-PCR.....	32
3.6. Functional analysis of differentially expressed genes using Faltigo plus and IPA.....	33
3.7. Statistical analysis.....	33
4. Results	34
4.1. Measurement of RBE of A549 cells.....	34
4. 2. RNA quality control.....	35
4.3. Pre-processing step of microarray data analysis.....	36
4.4. Identification of genes regulated significantly by carbon ion beam radiation.....	38
4.5. Gene networks and gene ontology analyses.....	38
4.5.1. Cellular functional classification of differently regulated gene.....	38
4.5.2. Genetic network and cellular functional classification of differentially regulated genes induced by carbon ion irradiation.....	39
4.5.3 Genetic network of the up- and down-regulated genes between carbon ion and X-ray irradiation.....	44
4.6. Validation of gene expression by qRT-PCR.....	55
4.6.1. Standard curves of primers used.....	55
4.6.2. Expression levels of irradiated genes.....	56
5. Discussion	62
5.1. Increased RBE of carbon ion beam on A549 cells.....	62
5.2. Gene expression profiling changes differently between X-ray and Carbon ion radiations.....	63
5.3. Signaling pathways of differently expressed genes between carbon ion irradiation and X-ray.....	64
6. Future prospects	67

7. Summary	68
7. Zusammenfassung	70
8. Reference	72
9. Appendix	86
9.1. List of figures.....	86
9.2. List of tables.....	88
9.3. Genes significantly up-regulated by carbon ion beam irradiation.....	89
9.4. Genes significantly down-regulated by carbon ion beam irradiation.....	91
9.5. List of genes up-regulated by carbon ion beam irradiation compared to X-ray.....	92
9.6. List of genes down-regulated by carbon ion beam irradiation compared to X-ray.....	99
9.7. Abbreviation.....	106
9.8. Curriculum Vitae.....	108
9.9. Publications.....	110
9.10. Academic teachers.....	111
9.11. Declaration	112
9.12. Acknowledgment.....	113

1. Introduction

1.1. Conventional treatment for lung cancer

Because of the most important avoidable cancer risk of huge tobacco consumption, approximately 100 million mortalities were associated with tobacco-caused diseases, including lung cancer, cardiovascular disease and stroke in the 20th century (Gandini et al., 2008).

Lung cancer is the disease of uncontrolled cell growth in the lung and 90% of cases are related to smoking (Hecht et al., 2009). Lung cancer remains the leading cause of cancer-related death in industrial countries and accounted for 30% of all male cancer deaths and 26% of all female cancer deaths in 2010 (Jemal et al., 2011). It is reported that approximately 80% of lung cancer cases are non-small cell lung cancer (NSCLC), including adenocarcinoma, squamous cell carcinoma or large cell carcinoma, and 40% of patients with NSCLC are with locally advanced and/or unresectable diseases (Rosell et al., 2006).

Nowadays, the standard approaches for the treatment of NSCLC are surgery, chemotherapy and radiation therapy. They can be used either alone or in combination depending on tumor size, location and histology (Jassem, 2007, Coory et al., 2008). Surgical resection is the major potentially curative therapeutic option for NSCLC in early stage (stage I and II), whereas inoperable early stage NSCLC is often treated by radiotherapy (Erman et al., 2004; Bogart et al., 2005, Scott et al., 2007). Chemotherapy combined with radiation therapy is commonly applied for NSCLC in advanced stages (stage III and IV). In last couple of decades, many approaches to multimodality therapy have been studied in patients with NSCLC. Modern technical development in radiation therapy including intensity modulated radiation therapy, image guided radiation therapy and more accurate dose calculation algorithms has been shown to improve local control of resected advanced NSCLC (Haasbeek et al., 2009). Unfortunately, the latter has failed to translate in an improvement in patient survival due to the frequent recurrence and metastases appearing even after aggressive treatment schedules (Rengan et al., 2011).

1.2. Charged particle beam radiation therapy

1.2.1. Charged particle radiation

One of the most important points during radiation therapy of cancers is to concentrate a precisely prescribed dose to the target volume while minimizing the dose to surrounding normal critical structures. The superior biophysical and biological profiles of particle beams such as carbon beam and protons with excellent dose localization and sparing of normal tissues make them highly attractive for treating malignant tumors including lung cancer (Kraft et al., 1998; Lomax et al., 2001, Chen et al., 2004, Fokas et al., 2009; Minohara et al., 2010)

Particle radiation is the radiation of energy by emitting of fast-moving subatomic particles, such as protons or ions, in the form of positively or negatively charged particles. Photons, neutrons and neutrinos are uncharged particles, while electrons, protons, alpha particles and heavier atomic ions are charged particles (Schulz-Ertner et al., 2007). The charged particle radiation therapy uses a wide range of different beams of protons or other charged particles, such as helium, carbon, neon, or silicon (Terasawa et al., 2009). In 1946, R. Wilson mentioned the advantage of Bragg Peak (Fig. 1) and proposed the clinical application of high energy protons and heavier ions in treating the deep seated tumor (Wilson, 1946). In 1948, R. Stone and J.C. Larkin used fast neutrons to treat patients with advanced incurable cancer in various sites (Stone, 1948). But the neutron trial was terminated because of severe side effects in spite of good tumor control rates. Pioneering clinical studies of particle radiotherapy were performed in 1950's to treat patients with proton and later on with helium ion at Lawrence Berkeley Laboratory in California (Tobias et al. 1952). Because of the prospective superiority of depositing the maximum energy at the range end with less scattering than when using conventional X-ray, carbon ion beams become one of the first candidates of substitutes for currently clinical use. The expanding interest in particle therapy has intensified the effort to better understand the particle irradiation both at the physical and the biological sides (Schulz-Ertner et al., 2007).

1.2.2. Biological advantages of charged particle radiation

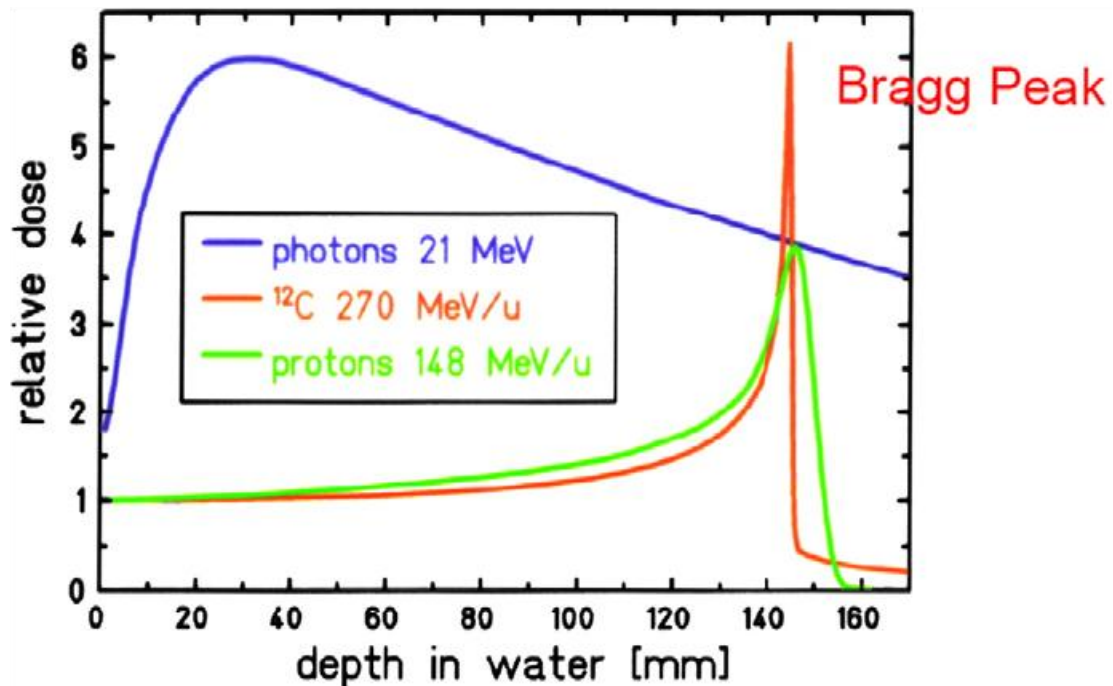


Fig. 1. Schematic diagram of Bragg Peak. The dose produced by a carbon ion beam and by a proton beam in passing through water, compared to the absorption of a photon beam (Fokas et al., 2009).

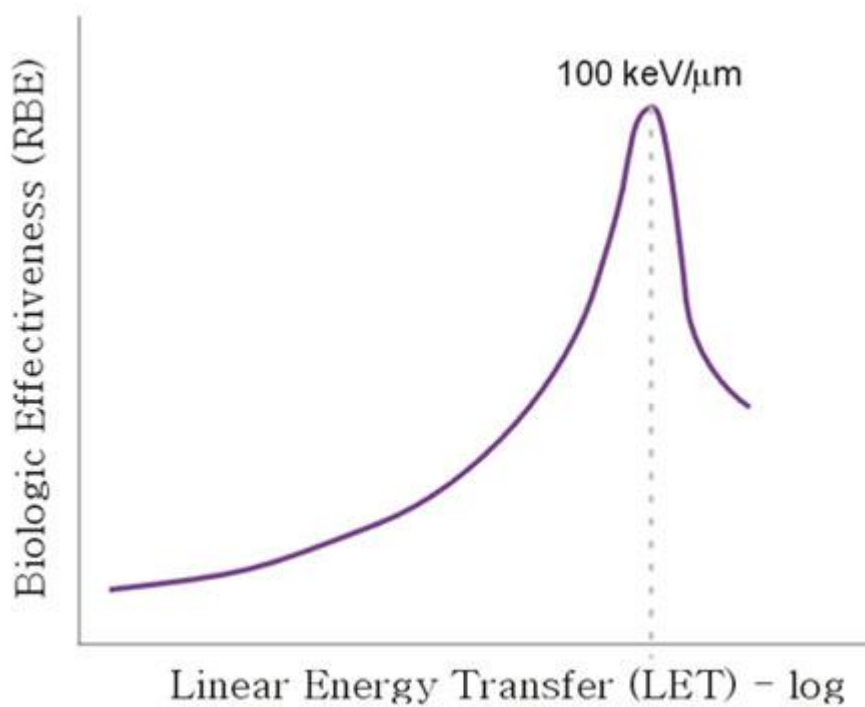


Fig. 2. Relationship of linear energy transfer (LET, 100 KeV/μm) and Relative Biologic Effectiveness (RBE) for carbon ions (Franken et al., 2011).

The conventional radiotherapy has been utilizing X-ray beams, which deposit the maximum dose within a few centimeters of the skin surface proximal to the intended target and continue to irradiate beyond the region targeted for treatment. Obviously, this energy distribution trajectory of X-ray beams has certain advantages in curing skin cancers, such as basal cell carcinoma, and malignant melanoma. However, tumors centrally located in the body could only receive 60 to 70% of the total dose administered with each individual X-ray beam, while the surrounding tissues were unavoidably affected (Fokas et al., 2009).

Thanks to its superior physical properties, irradiation therapy using high-energy charged beams, such as carbon ions, have several advantages when compared with the conventional irradiation with photons.

1). Charged particle beam has higher relative biological effectiveness (RBE)

A major concept in estimating the efficacy of charged particle beams is RBE. The RBE is defined as the ratio of the absorbed doses of two different radiation beams required that results in the same biological effect. The RBEs between different radiation beams are varied, depending on many parameters, including the biological endpoint, fractionated dose, particle type and energy, as well as the oxygenation status of tissue irradiated (Weyrather et al., 2004). Therefore, the RBE is patient specific in every location in the treatment fields and has to be precisely calculated by sophisticated scientists prior to clinical practice.

Another concept to define the ionizing density along a particle track is linear energy transfer (LET). The conventional photon beams deposit most of their energy near the surface (skin and normal tissues in clinical therapy) and decrease in the dose profile with depth when going through matters (e.g. normal tissues beyond the tumor). In contrast, charged particle beam exhibits a LET, which penetrates with increasing depth and reaches a maximum in the Bragg peak region (Kraft, 1998).

Carbon ions and neutrons are high-LET beams, when compared to the low-LET proton and photon beams, thus, under the same circumstances, heavier ion beam with higher-LET shows higher RBE (Bassler et al., 2010).

2). Charged particle beam causes more severe damage to cells

Since the very beginning of the 19th century, abundant studies had reported the harmful effects of radiation. Low-LET radiations can cause cellular damages to nucleotide bases,

cross-linking, DNA single- and double-strand breaks (DSBs), and genomic instabilities. Base excision repair and nucleotide excision repair are the common ways for individual cells to recover its functions (Goodhead et al., 1993; Eckardt-Schupp et al., 1999). Charged particle beams cause more severer DNA damages, known as clustered damage, which is difficult, even impossible, to repair (Goodhead, 1994). Previous studies showed that after high-LET beam irradiations, at least 70% of DSBs caused contain more than two breaks and show higher complexity than with low-LET beams (Kraft et al., 1992; Goodhead, 1999). When DNA damage heavily clustered, the repair of base damage become relative slow and can create further DSBs, which can lead to possible linkage on different chromosomes and derive molecular inventories (Dianov et al., 2001; Singleton et al., 2002).

3) Charged particle beam exhibits lower oxygen enhancement ratio (OER)

As a tumor grows, the oxygen concentration in the tumor region is usually lower than in the normal tissue area, which is due to the great oxygen demand to support the rapid tumor growth. Tumor hypoxia is a well-recognized factor contributing to tumor progress, angiogenesis and genetic instability and is one of the limiting factors in cancer radiotherapy (Bassler et al., 2010). The OER is the ratio of radiation dose in the absence of oxygen to the dose in the presence of oxygen required for the same biological effect. Previous studies of OER found that the OER for conventional radiation therapy with photons is much higher (about 3) than the OER for heavy ions (only 1.5 to 1.8) (Skarsgard, 1998; Furusawa et al., 2000). The potential of carbon ion radiotherapy in overcoming hypoxia-induced resistance has been demonstrated in clinical study of cervical cancer (Nakano et al., 2006). This trial involved cervical cancer patients treated with a 400 MeV per nucleon carbon ion beam. The similar disease-free survival and local control between hypoxic and oxygenated tumors indicated that the role of the tumor oxygenation status was not important in carbon ion therapy.

The superior biophysical and biological profiles of carbon beam radiation with high-LET of excellent dose localization, high biological effect and sparing of normal tissues, make it highly attractive for treating malignant tumors including lung cancer.

1.2.3. Charged particle radiation applied in cancer therapy

The pioneering clinical studies of charged particle therapy can go back to 1950s, which were performed at accelerators built for physics research (Tobias et al. 1952). But the first hospital-based proton facility was commissioned in 1990 at the Loma Linda University Medical Center in USA and the first hospital-based heavy ion facility was constructed in 1993 at National Institute of Radiological Sciences in Japan (Gademann et al., 1990, Hirao 1992, Schulz-Ertner et al., 2007). Parallel to the continuously development in the field of the facilities, that provide X-rays, electrons, light and also heavy ions, the interest of charged particle therapy of cancer have been increasing substantially all over the world within the last two decades. Nowadays, ion irradiation using protons and heavier ions such as carbon beams are widely applied both experimentally and clinically (Pijls-Johannesma et al., 2008). Until end 2010, approximately 84,900 patients have been treated worldwide with particle radiotherapy. Of them, about 6,660 patients have received carbon ion therapy in Japan and Germany (PTCOG, 2010).

Carbon ion radiotherapy showed a specific effectiveness in local control of different types of cancer. Between 1994 and 2005, 2,371 patients with malignant tumors were registered in phase I/II dose-escalation studies and clinical phase II trials using hypofractionated carbon ion therapy. Compared with conventional radiotherapy, carbon ion beams can reduce the overall treatment times and also achieve better local tumor control, even for radio-resistant tumors such as malignant melanoma, hepatocellular carcinoma and bone/soft tissue sarcomas with minimal morbidity to the normal surrounding tissues (Ishikawa et al., 2006; Okada et al., 2010).

1.2.4. Charged particle radiation applied in NSCLC

Carbon ion therapy has also been investigated in the patients suffering from NSCLC. In a prospective nonrandomized phase I to II trial in Japan, different dose fractionation scheme for carbon ion has been tested in 81 patients with stage I NSCLC, who were not candidates for surgical resection. The optimum safety and efficacy dose were investigated by conducting different radiation fractions and dose escalation methods to two groups of patients. The optimal dose of carbon ions was determined to be 68.4

79.2 GyE (photon gray equivalents) administered in 9 fractions. The five-year local control and overall survival rate were 84%, and 45%, respectively (Kadono et al., 2002, Miyamoto et al., 2003). Proton radiation therapy using 50-76 GyE in 10 or 20 fractions in clinical trials has received five-year local control rates of 89% and 39% for stage IA and stage IB NSCLC, respectively. The overall survival rates for these two groups were 70% and 16%, respectively (Shioyama et al., 2003, Nihei et al., 2006). A recently reported meta-analysis compared the treatment effectiveness of photon, proton and carbon radiation therapy. The results demonstrated that five-year overall survival for conventional radiotherapy (20%) was statistically significantly lower than that for stereotactic radiotherapy (42%), proton therapy (40%) and carbon-ion therapy (42%) (Grutters et al., 2010).

Several research groups have performed evaluations of the tumor response and the side effects of patients NSCLC after carbon ion therapy. Miyamoto et al. (2003) reported in 3.7% of the patients had acute side effects (grade 3 and more) and 1.2% had late side effects (grade 3 and more). In the recently published phase I/II trial of the same investigators were a total dose of 52.8–60 GyE was delivered over 1 week, no grade 3+ acute or late toxicity was observed. These clinical data indicated that carbon ions therapy can especially reduce late side effects and is safe and feasible in the treatment of NSCLC (Miyamoto et al., 2003, Pijls-Johannesma et al., 2008). However, randomized trials to compare different techniques of radiation therapy are needed to clarify the application of carbon ions radiation therapy in NSCLC in advanced stage.

1.3. Gene expression changes induced by irradiation

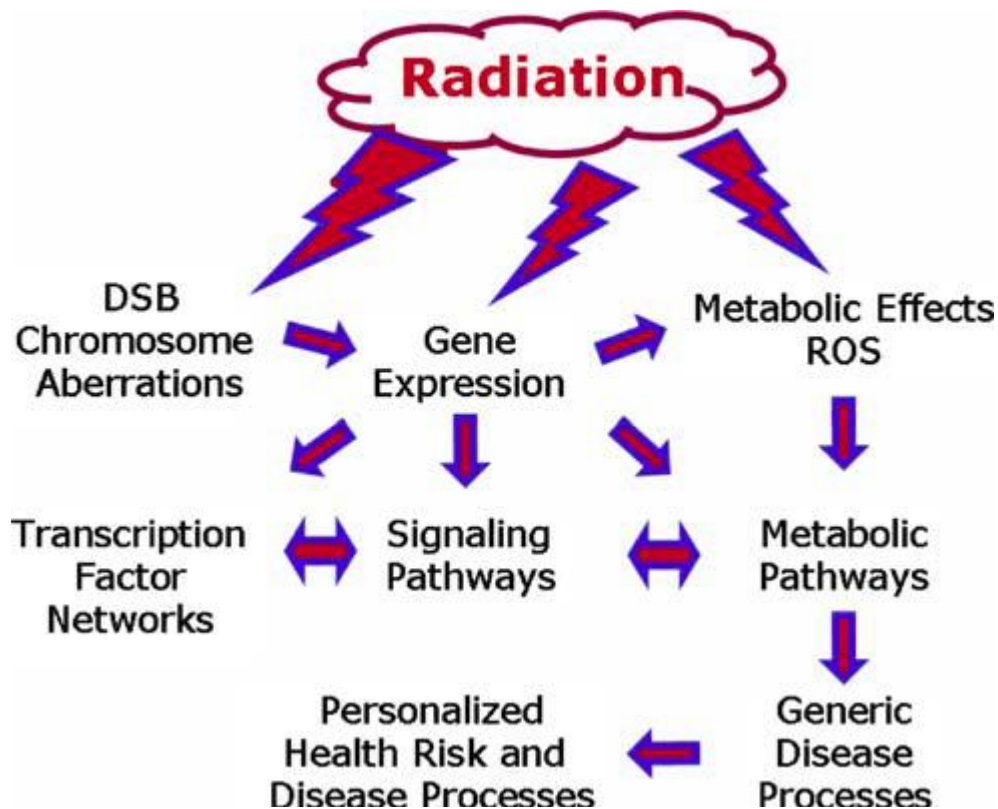


Fig.3. Radiation induced a series of biological responses progressed in different levels (Feinendegen et al., 2008)

DNA DSB is thought to be the lethal lesion caused by ionizing radiation and can result in rearrangement of genetic information, leading to cell death or carcinogenesis. DNA damage includes activation of a number of signal transduction cascades and stimulates several components in concert to activate the cellular checkpoint, which leads to cell cycle delay, DNA repair and programmed cell death (Jeggo et al., 2006). The alterations in gene expression also represent a central component of the pathways involved. Studies of altered gene expression have historically played an important role in elucidating the molecular mechanisms underlying cellular radiation response (Eckardt-Schupp et al., 1999; Feinendegen et al., 2008).

1.3.1. Gene expression changes induced by X-ray

Several studies of X-ray interactions in DNA have provided evidence for DNA damage which also has a high probability of producing DSBs. These cellular changes may initiate neoplastic transformation of the cell and diverse effects on differentiation and growth (Nakano et al., 1994). The primary studies of the progressive nature of carcinogenesis were predicted *in vivo*. Since 1978, *in vitro* transformation system has been used to study the molecular mechanism of multistep carcinogenesis (Barrett et al., 1978).

After exposure to radiations, cell cycle delay is often found in mammalian cells. It is generally hypothesized that this delay provides damaged cells additional time to self-repair before the cell enters critical periods of the cell cycle (Murnane, 1995). It is widely known that CDKN1A (p21) protein is an inhibitor of cyclin-dependent kinases (CDK), a family of protein kinases known as key regulators of cell cycle progression. Never the less, CDKN1A can inhibit several CDK and most effective toward G1/S cyclins. Other CDK inhibitors, such as CDKN1B (p27) and CDKN2B (p15) are activated by irradiation and contribute to the G1 arrest. Moreover, radiation-induced G2 arrest was shown to require inhibitory phosphorylation of the kinase CDC2 via an ATM (ataxia telanictasia mutated)-dependent pathway (Abbas and Dutta, 2009). The expression of CDKN1A protein after exposure to irradiations is generally accepted as an indicator of cells with a wild-type p53 (Nakano et al., 1994). Radiation induced DNA DSB often lead to the activation of p53 through ATM pathway and to induce apoptosis (Banin et al., 1998).

Hennes et al. reported that fractionated X-ray treatment alone can produce increased radiation and drug resistance in SCLC cells, which was due to the decreased expression of BCL2 and glutathione-S-transferase- π and increased expression of multidrug resistance-associated protein 1 (MRP1), MRP2, N-myc and topoisomerase-II α (Hennes et al., 2002). The CGRP (calcitonin gene-related peptide) and substance P, the two major neuropeptides released by sensory neurons, are overexpressed after irradiation and have opposing effects during development of intestinal radiation injury (Wang et al., 2006). Down-regulation in response to low dose X-ray (0.1-0.3 Gy) was observed in mRNA level of CDC2, cyclin A, cyclin B, thymidine kinase, topisomeras IIa, and RAD51 (de Toledo et al., 1998).

1.3.2. Gene expression changes induced by heavy ion beams

Although heavy ion have been applied in clinical therapy of cancers for many years, the genetic mechanisms and the signaling pathways involved in cellular responses to heavy ion radiation are not completely understood. Several previous studies have evaluated the correlation between cellular responses to carbon ion irradiation and the expression status of known genes involved in the regulation of cell cycle, DNA repair, and apoptosis using analytical approach for single gene. Recent studies demonstrated that irradiation with carbon beams induced not only apoptosis, but also cellular senescence in glioma cells with either wild-type or mutant p53 expression, more effectively than X-ray (Guida et al., 2005; Jinno-Oue et al., 2010). Using semiquantitative real time PCR, significant different expressions of 10 selected genes involved in DNA repair have been showed to be responsible to inhibition of potential lethal damage repair in cultured lung cancer cells after carbon ion irradiation compared to X-ray (Yashiro et al., 2007). The expression and focus formation of CDKN1A, a member in the complex of MRE11/RAD50/NBS1 ensuring DSB repair, is correlated with the traversal of ionizing particles (Jakob et al., 2002). Through pathological investigation and immunohistochemical analysis of CDKN1A, carbon ion has been found to be responsible for cell cycle arrest in tumor cells with mitotic catastrophe (Imadome et al., 2008). Recent study using a cDNA expression array containing 161 key genes in damage and repair signaling pathway has revealed that 38 and 24 genes were differentially altered in breast epithelial cell treated with X-ray and heavy ion (Fe^{+2}), respectively (Roy et al., 2008).

Microarray technology are currently used to investigate gene expression profile in cancer cells and tumor samples exposed to heavy ions irradiation, but only few exist to date. Using single-color oligo-microarrays, Nojiri et al. (2009) compared the gene expression profiles of two murine squamous cell carcinomas, which are respectively highly radioresistant and radiosensitive. After irradiation with X-ray or carbon ions, 4 genes, EFNA1, SPRR1A, SRGAP3 and XRRA1 were identified associated with the character of radioresistant. In a microarray study of oral squamous cell carcinoma (OSCC) cells, 84 genes were greatly modulated after exposure to carbon ions. Of these regulated genes, three genes (TGFB2, SMURF2, and BMP7) and two genes (CCND1 and E2F3), respectively, were found to be involved in the transforming growth factor

beta-signaling pathway and cell cycle:G1/S checkpoint regulation pathway. (Fushimi et al., 2008). In a similar study on oral squamous cell carcinoma cells, a set of 98 genes was modified after carbon ions irradiation and remained unchanged in their expressions after X-ray irradiation. However, clustering analysis of expression profiles among metastatic tumors in murine model has showed little difference in nonirradiated, carbon ion irradiated, and γ -ray irradiated groups, while same pathologic findings have gained among these groups (Tamaki et al., 2009).

1.4. Modern technologies applied in studying of gene functions

Many years of intensive research have demonstrated that the signaling molecules of encoded genes with various functions are organized into complex biochemical networks. These signaling circuits are complicated systems consisting of multiple elements interacting in a multifarious fashion. Actually, the analysis and determination of unknown genes interactions as well as their association with diseases often contain screening of hundreds of thousands of transcripts and meaningful predictions of sound computational algorithms (Li et al., 2009). Therefore, more efficient solutions are in urgent need for genetic research.

The development of automated methods for the study of gene functions is becoming an increasingly important area of investigation in bioinformatics and computational biology. High-throughput methods such as microarray, allow researchers to perform millions of biochemical, genetic or pharmacological tests rapidly and simultaneously. The characteristics of cost-effective and high throughput technology are the combination of analytical robotics, data processing and control software, liquid handling devices and sensitive detectors (Hertzberg et al., 2000).

1.4.1. Microarray technology in biomedical and clinical research

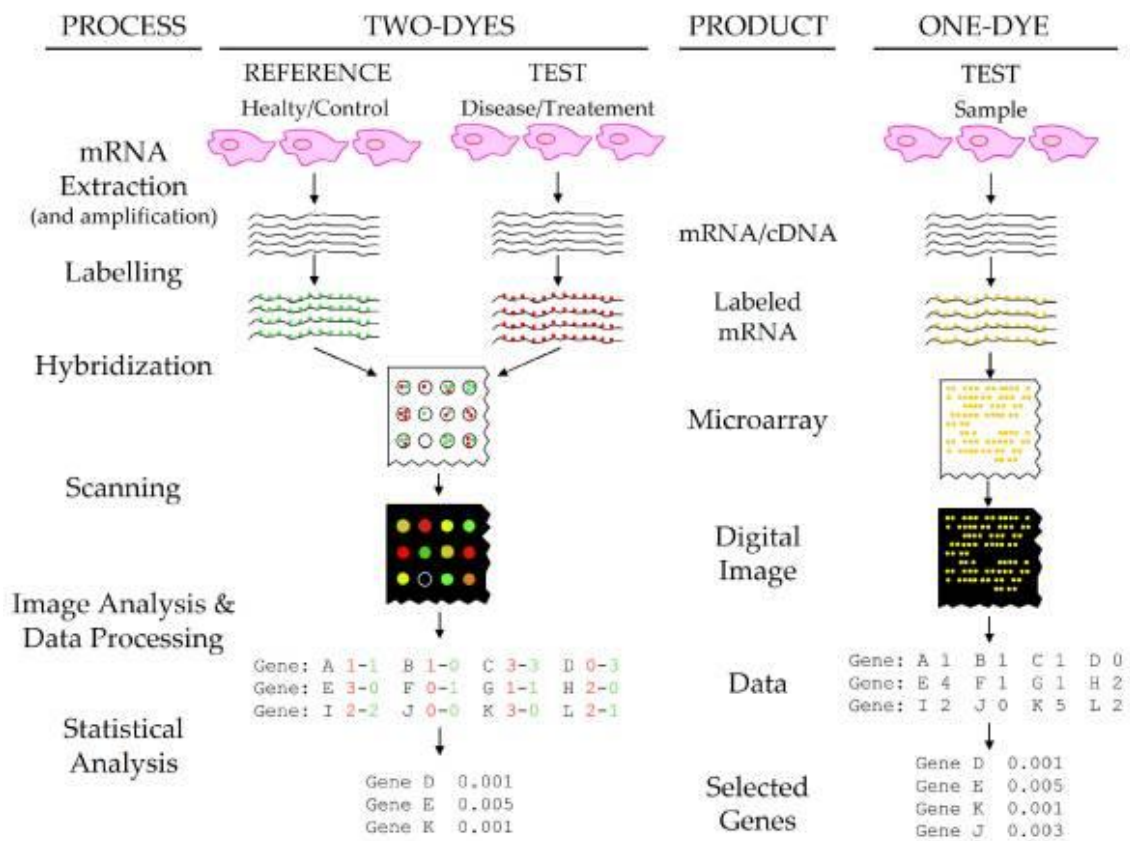


Fig. 4. Schematic representation of microarray assay of gene expression

As shown in Fig. 4, microscopic arrays of large sets of cDNA sequences or oligonucleotides immobilized on solid substrates are multiplex lab-on-a-chip, which can analyse hundreds of thousands of biological materials simultaneously via high-throughput screening methods (Bhattacharya et al., 2009). Nowadays, microarray technology has been applied for comparing genome features among individuals and their tissues and cells, and has become one of the standard tools of high-throughput analysis in all the aspect of biomedical research (Trevino et al., 2007).

With this technology it is possible to analyse gene expression patterns for studying the genetic changes of tumor progression, the cellular response to chemo- and radiation therapy, and drug target identification. According to the published data, many tumor subtypes can be identified in reference to the variations (increased or decreased) of gene expression or changes in transcriptional profiles (Alizadeh et al., 2000, Kikuchi et al., 2003, Nagata et al., 2003, Ramaswamy et al., 2003, van't Veer et al., 2008). Moreover, recent studies showed that the utilizes of microarrays are fully widen to detecting single

nucleotide polymorphisms, aberrations in methylation patterns, alterations in gene copy-numbers, alternative RNA splicing and also pathogen detection, but not only limited to gene expression.

1.4.2. Microarray technology applied in lung cancer research

The high-throughput microarray analysis of gene expression has been systematically used to examine differentially expressed genes, and molecular pathways and to identify tumor markers of lung cancer.

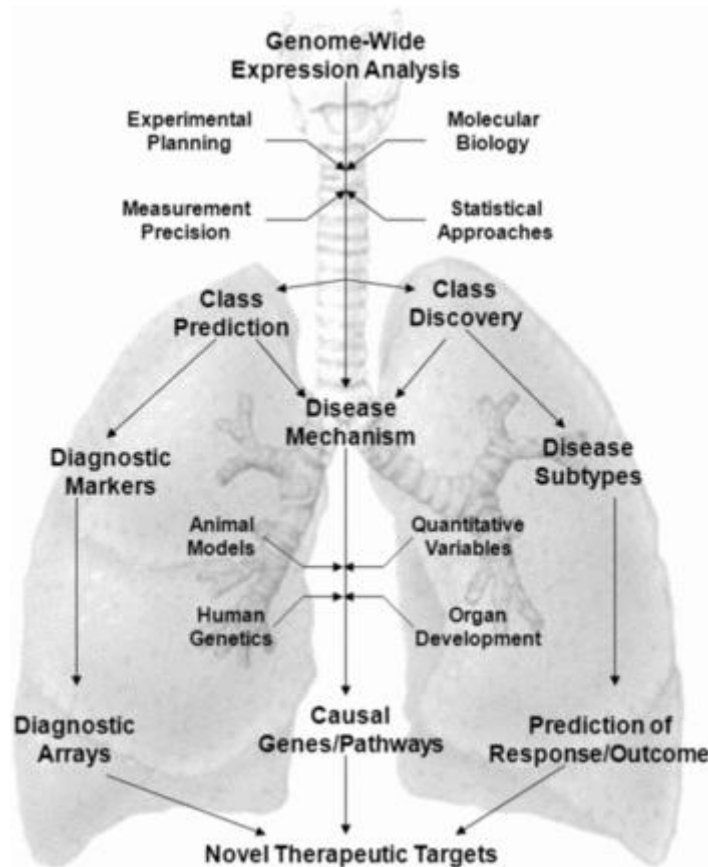


Fig. 5. Overview of the utility of gene expression microarray technology in lung cancer for discovery of tumor marker and therapeutic target

Using oligonucleotide microarrays consisting 12,600 transcript sequences, Bhattacharjee et al. (2001) generated a molecular taxonomy of 186 lung carcinomas including 139 adenocarcinomas and defined distinct subclasses of lung adenocarcinoma by hierarchical and probabilistic clustering of gene expression. To identify low- and high-risk individuals, Beer et al. (2002) analysed a data set of 4,966 genes in 86 lung

adenocarcinomas and built a risk index of the top 50 genes by using two equivalent but independent training and testing sets. Microarray analysis has been used to predict clinical outcome of patients with lung cancer and to determine patients for aggressive therapies. By studying a cohort of 86 patients with lung adenocarcinoma, Guo et al. (2006) created a 37 gene signature using several bioinformatics tools. The gene signature was used to predict the survival of these patients by Kaplan-Meier analysis. These patients could be classified into three groups with good, moderate and poor prognoses based on the gene expression profiles. Moreover, several groups have evaluated gene expression profiles of lung cancer to predict the response to chemotherapy and radiation therapy. The gene signature profile identified by Potti et al. (2006) predicted recurrence for 89 patients with early stage NSCLC after adjuvant therapy significantly better than conventional prognostic factors. These microarray studies provided potential clinical applications of gene expression profile in field of differentiating diagnosis, prediction of treatment outcome of patients and discovery of novel tumor markers for molecular therapy of lung cancer.

1.4.3. Gene expression profiling using microarray technology in cancer research

Grouping genes based on functional similarities can systematically enhance biological interpretation of large lists of genes derived from high throughput studies, such as cDNA microarray analysis (Streit et al., 2009). The most frequent employment of microarray in cancer research was to compare gene expression profiling between cells with different sensitivity to treatments, including radiation or drugs (Hellman et al., 2005, Poulsen et al., 2005). In clinical researches, microarray has also been applied to test the tumor proliferations in more than 1,000 patients with various tumors (Starmans et al., 2008).

Once upon a time, categorizing of tumors was only based on histological classification of cancer samples. Using various microarray chips, the signature of a tumor from an individual patient can be diagnosed conveniently (Liotta et al., 2000). As of today, more than a dozen studies evaluating lung cancer using DNA microarray technologies as well as a meta-analysis have been published (Lu et al., 2006, Liang et al., 2008).

Although there are many platforms for profiling cancers, including mass spectrometry,

antibody arrays (Ostroff et al., 2010) and methylome profiling (Heller et al., 2010), the most common methods are microarray chips analysis and qRT-PCR validation afterwards (Singhal et al., 2008).

1.5. The aim of this study

This study is a cooperation of the GSI (Gesellschaft für Schwerionenforschung) Darmstadt and the Philipps-University Marburg. The main goal of this study is to increase understanding of the response of NSCLC to heavy ion irradiation. In order to achieve this objective, human lung adenocarcinoma cell line A549 was used for analysis of the gene expression profiles induced by X-ray and carbon ion irradiation in this study.

The study includes specific goals,

- 1). Determine the clonogenic survival ability of A549 cells after exposure to X-ray and carbon ion irradiation using colony forming assay,
- 2). Compare the RBE of X-ray and carbon ion irradiation in A549 cells,
- 3). Optimize the experimental conditions for microarray analysis of A549 cells,
- 4). Determine and compare the gene expression changes induced by X-ray and carbon ion irradiation,
- 5). Classify the differently changed genes according to the biological functions and analysis the signaling network among them,
- 6). Optimize the quantitative methods of gene expression changes in A549 cells,
- 7). Validate these differently changed genes

2. Materials

2.1. Cell line

The human lung adenocarcinoma cell line A549 was purchased from the American Type Culture Collection (ATCC, Manassas, VA). The cells were derived through explant culture of lung carcinomatous tissue from a 58-year-old Caucasian male (Giard et al., 1973).

2.2. Primers

Table.1. Primer sequences and PCR conditions.

Gene	Entrez Gene ID	Forward primer (5'-3') Reverse primer(5'-3')	Product Size (bp)
CCND2	894	TACCACTATGGGGTCAGC GTGGCCACCATTCTGCGC	181
CDCA5	113130	CATCTCCTACTAAGCCTCTGCG CGATCCTCTTTAAGACGATGGG	132
CDC14B	8555	GTGCCATTGCAGTACATT AGCAGGCTATCAGAGTG	123
CDC25B	994	CCGCTCAAATCACTGTGTCA GCTCTTCAGTAGGAAGCTCTCG	298
CDKN1A	1026	CCTGTCACTGTCTTGTACCCT GCGTTTGGAGTGGTAGAAATCT	130
E2F5	1875	TCAGGCACCTTCTGGTACAC GGGCTTAGATGAACTCGACTC	145
RARG	5916	TACCACTATGGGGTCAGC CCGGTCATTTTCGCACAGCT	195
TP53I11	9537	ATCAGCCAGGTCTTAGGCAAT GCCGTGTAGAGCGTTCC	242
GAPDH	2597	TGGTCACCAGGGCTGCTT AGCTTCCCCTTCTCAGCCTT	150

2.3. Chemicals

ABsolute SYBR Green Mixes	ABgene, Germany
Agarose	Sigma Aldrich, Germany
Ampicillin	PAA, Germany
DEPC	Sigma Aldrich, Germany
Distilled water	Millipore, Germany
DMSO	Sigma Aldrich, Germany
DNase I, RNase-free	Fermentas, Germany
dNTPs	Fermentas, Germany
EDTA	AppliChem, Germany
Ethanol 100%	Roth, Germany
GeneRuler 100bp DNA ladder	Fermentas, Germany
Glacial Acetic Acid	Sigma Aldrich, Germany
HEPES	Sigma Aldrich, Germany
6 × loading dye solution	Fermentas, Germany
Methylene blue	Fermentas, Germany
MgCl ₂	Fermentas, Germany
M-MuLV reverse transcriptase	Fermentas, Germany
NaCl	Sigma Aldrich, Germany
Na ₂ EDTA•2H ₂ O	Sigma Aldrich, Germany
NaOH	Sigma Aldrich, Germany
PBS buffer	PAA, Germany
Penicillin/streptomycin	PAA, Germany
Ribonuclease inhibitor	Fermentas, Germany
RPMI 1640 medium	PAA, Germany
Sodium Citrate	Sigma Aldrich, Germany
Taq-polymerase	Fermentas, Germany
Tris Base	Sigma Aldrich, Germany
Trypsin/EDTA	Invitrogen, Germany

2.4. Experiment Kits

CyScribe cDNA Post Labeling Kit	Amersham Biosciences, Germany
DNeasy blood & tissue kit	Invitrogen, UK
First Strand cDNA synthesis kit	Fermentas, Germany
MessageAmp aRNA Kit	Qiagen, Germany
PCR Purification Kit	Qiagen, Germany
RNeasy mini kit	Qiagen, Germany

2.5. Reagents

Bovine serum albumin	PAA, Germany
Fetal bovine serum (FBS)	Sigma, Germany
Penicillin/streptomycin	PAA, Germany
RPMI 1640	PAA, Germany

2.6. Consumables

1.5 ml Eppendorf centrifuge tubes	Eppendorf, Germany
15 ml Polypropylene tubes	FALCON [®] , NJ, USA
3.5 cm Petri dishes	Roth, Germany
25 cm ² T cell culture flasks	Nunclon [™] , Denmark
iQ 96-well PCR plates	Bio-rad, USA
96-well PCR Plate Sealing Mates	Bio-rad, USA
10 µl white tips	Roth, Germany
200 µl yellow tips	Roth, Germany
1000 µl blue tips	Roth, Germany
Distilled water	Millipore, Germany

2.7. Apparatus

-20 °C Refrigerator	Bosch, Germany
-80 °C Refrigerator	Bosch, Germany

37 °C CO ₂ incubator	Heraeus, Germany
Coulter Counter Z2	Beckman, U.S.A
Elekta SL-25 linear accelerator	Norcross, GA
GMS 417 arrayer	MWG Biotech, Germany
G148 microarray scanner	MWG Biotech, Germany
Heating block	VWR, Germany
iCycler	Bio-Rad, USA
Laminar flow cabinet	Heraeus, Germany
Pipettes	Eppendorf, Germany
Shaking incubators	Heraeus, Germany
Table centrifuge	Heraeus, Germany
UV spectrophotometer	Bio-Rad, USA
Water bath	Lauda, Germany

2.8. Buffers and medium

0.5 M EDTA (pH=8)

186.1 g Na₂EDTA•2H₂O (MW=372.24)

Dissolve EDTA in 800 ml ddH₂O. Adjust pH with NaOH pellets (about 20 g). Bring the whole volume to 1000 ml with ddH₂O. Sterilize by autoclaving and store at room temperature.

2 M HEPES

476.6 g HEPES

Dissolve HEPES in 800 ml ddH₂O. Adjust pH with 4 N NaOH solution. Bring the final volume to 1000 ml with ddH₂O. Store at 4 °C.

20 × SSC (pH= 7.0)

175.3 g NaCl

88.2 g Sodium Citrate (Na₃C₆H₅O₇•2H₂O)

Dissolve all the salts in 800 ml ddH₂O, stir till all solid dissolved. Use a few drops of 25% HCl to adjust the pH, and then bring the final volume to 1000 ml with ddH₂O.

Sterilize by autoclaving and store at room temperature.

50 × TAE Buffer (1L)

242 g Tris Base

57.1 ml Glacial Acetic Acid

100 ml 0.5 M EDTA (pH=8)

Mix Tris Base and approximately 600 ml ddH₂O, stir till all solid dissolved. Add glacial acetic acid and EDTA solution to the mixture. Bring the whole volume to 1000 ml with additional ddH₂O. Stir to make it even and store at room temperature.

Cell culture medium

450 ml RPMI 1640

50 ml Fetal bovine serum (FBS)

5 ml Penicillin/streptomycin

Mix the three reagents together inside the clean bench and store in the 4 °C.

Cell frozen buffer (10 ml)

1 ml DMSO

2 ml FBS

7 ml RPMI 1640

Mix them together inside the clean bench and store at 4 °C.

3. Methods

3.1. Cell cultures

3.1.1. Thawing cultured cells

A549 cell line was stored in 1.8 ml freezing tubes in liquid nitrogen before use. The cells were thawed quickly in 37 °C water bath and then transferred to a sterile 15 ml tube containing 5 ml preheated RPMI 1640 medium supplemented with 10% FBS and 1% penicillin-streptomycin. Following centrifugation at 1800 rpm for 3 min, the cells were resuspended in T-25 cm² flask containing 5 ml preheated culturing medium. The flasks were incubated at 37 °C in a humidified 5% CO₂ atmosphere until the cells reached confluence.

3.1.2. Trypsinizing and subculturing cells

After complete aspiration of culturing medium, A549 cells were washed with PBS and trypsinized with 1 × trypsin-EDTA solution. Culturing medium was added into the flasks once all the cells were detached from the flask. Then the floating cells were transferred to a 15 ml centrifuge tube. Following centrifugation at 1800 rpm for 3 min, the cells were resuspended in fresh medium and seeded into a new flask. The medium was replaced 2 to 3 times per week.

3.2. Radiation

Cells were reseeded in 3.5 cm Petri dishes 24 hours before irradiation to gain a confluence of 70-80%. A549 cells were irradiated in special containers, which hold those culture dishes in a vertical position with the amount of cell culture medium needed to keep the dishes submersed. Conditioned medium was removed from the dishes of cell monolayers just prior to irradiation.

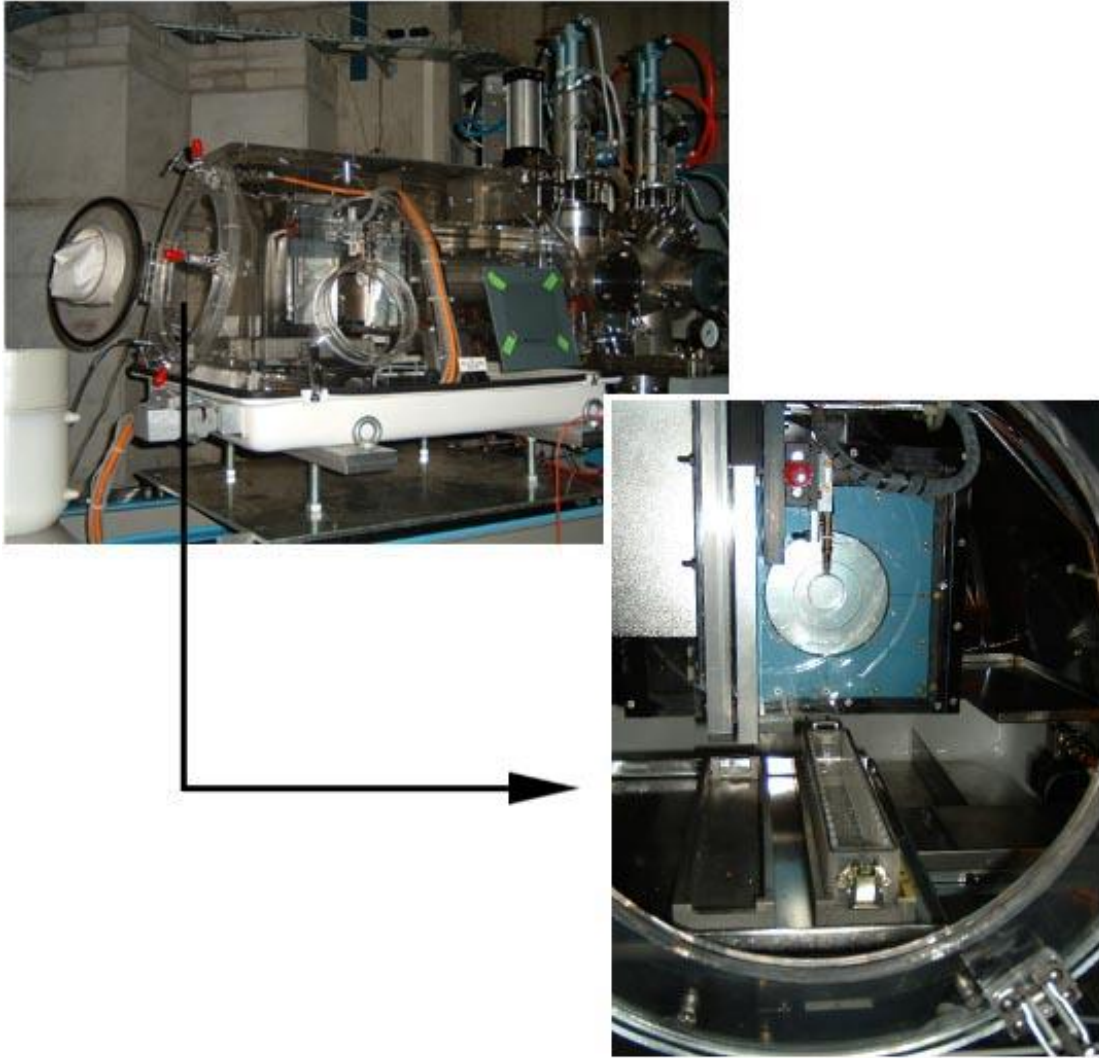


Fig.6. BIBA (Biologische Bestrahlungs-Anlage) facility in GSI, Darmstadt. 3.5 cm Petri dishes were placed in the magazine filled with cell culture medium, and irradiated in a vertical position perpendicular to the beam.

Irradiation with carbon ion (9.8 MeV/nucleon on target, LET 170 KeV/ μm , dose range from 0 to 6 Gy) and X-ray (250 kV, 16mA, dose range from 0 to 12 Gy) was performed at the UNILAC facility at GSI, Darmstadt, Germany. During carbon ion irradiation the Petri dishes were kept in a vertical position perpendicular to the beam (Fig. 6) as described previously (Conrad et al., 2009). Cells were reseeded in 25 cm² T flasks immediately after irradiation and collected at different time points for further analysis.

3.3. Colony forming assay

The RBE of high-LET radiation, such as carbon ions, is higher than that of X-ray (Ohnishi et al., 2004). In order to determine the biological equivalent dose between carbon ion and X-ray used in this study, colony forming assay was performed as described previously (Fournier et al., 2004). Briefly, A549 cells were trypsinized after irradiation and counted by Coulter Counter Z2 (Beckman, U.S.A). Samples from each time point and each dose were reseeded in 25cm² T flasks and incubated at 37 °C. The number of cells in each sample was determined with the respect to the planting efficiency and doses to obtain 100 colonies in final. After 14 days of incubation, all the samples were stained with Methylene blue for 10 min and observed under a microscope. Colonies formed by more than 50 cells were scored as survivors. All experiments were conducted in triplicate.

3.4. Microarray analysis

3.4.1. RNA-extraction

Total RNA was extracted from frozen cell pellets using RNeasy Mint Kit (Qiagen, Germany) according to the manufacturer's instructions. In brief, completely thawed cell pellets were disrupted by adding 350 µl buffer RLT. Then, 1 volume of 70% ethanol was added to homogenized lysate and together they were transferred to an RNeasy spin column placed in a 2 ml collection tube. After centrifuged for 15 s at 13,000 rpm, the flow-through was discarded. This was followed by washing once with 700 µl of buffer RW1, and twice with 500 µl of buffer RPE for 15 s at 13,000 rpm. The RNeasy spin column was replaced in a new 1.5 ml collection tube. The RNA was eluted in 50 µl of RNase-free water by centrifugation for 1 min at 16,000 rpm.

3.4.2. Quantitative and qualitative analysis of RNA

The concentration of extracted RNA was determined photometrically at $\lambda = 260$ nm. The absorption of 1 corresponds to 40 μg RNA/ml for normal preparations (Sambrook et al., 1989). In addition, the A260/A280 ratio is an indication for RNA purity. Sufficiently pure RNA preparations showed a ratio higher than 1.8, whereas ratios lower than 1.8 indicate contamination with protein or phenol.

The integrity of purified RNA was checked by agarose gel electrophoresis upon ethidium bromide staining. The RNA samples were incubated in 37 °C water bath for 1 h. After incubation, RNA sample were mixed with 4.5 μl of water and 1 μl of freshly prepared loading buffer (6 x). The sample mixture was loaded on 1% agarose gel contained ethidium bromide (0.5 $\mu\text{g}/\text{ml}$) and separated by electrophoresis at 80 V for 1-2 h. The gels were then visualized under UV transillumination.

3.4.3. RNA amplification

In order to prepare sufficient RNA materials for array hybridization, the extracted total RNA samples were amplified using the MessageAmp aRNA Kit (Invitrogen, Huntingdon, UK) according to the manufacturer's manual. In brief, reverse transcription was done with an oligo (dT) primer bearing a T7 promoter using ArrayScript reverse transcriptase to produce full-length first-strand cDNA. The cDNA samples were undergone with second-strand synthesis and cleanup to become the template for in vitro transcription. Multiple copies of RNA sample were synthesized by T7 RNA polymerase and followed by one step of clean up. 10 to 50 μg mRNA has been amplified from 1 μg total RNA after one round of in vitro transcription.

3.4.4. cDNA synthesis

All RNA samples were subjected to DNase I (Fermentas, Germany) digestion for 30 min at 37 °C in order to prevent genomic DNA contamination. First strand cDNA synthesis was performed using cDNA synthesis kit (Fermentas, USA). Briefly, one microgram of total RNA was used for synthesis reaction containing 1 μl of oligo (dT)₁₈ primer (0.5 $\mu\text{g}/\mu\text{l}$) and DEPC-treated water to final volume of 11 μl and incubated at

70 °C for 5 min. Subsequently, 4 µl of 5 × reaction buffer were added together with 1 µl of RiboLock™ Ribonuclease inhibitor (20 u/µl). After incubation at 37 °C for 5 min, 2 µl M-MuLV Reverse Transcriptase (20 u/µl) were added to make a final volume of 20 µl. The mixture was finally incubated at 37 °C for 1 h followed by 10 min in 70 °C for inactivation of reverse transcriptase.

3.4.5. cDNA labeling

The cDNA samples were labeled with Cy3 and Cy5 dyes, using the CyScribe cDNA Post Labeling Kit (Amersham Biosciences Europe, Freiburg, Germany). Briefly, RNA samples (3 mg) were reverse transcribed with nonamer primers, incorporating modified amino-allyl-dUTP. The synthesized cDNA was denatured with 2 µl NaOH (2.5 N) at 37 °C for 15 min, followed by neutralization with 10 µl HEPES (2 M). The labeled cDNA samples were purified using PCR Purification Kit (Qiagen, Hilden, Germany) to remove unbound Cy dyes.

3.4.6. Microarray experiments

Microarray hybridizations were performed at the Institute of IMT (Molecular Biology and Tumor Research), Philipps-University Marburg as described previously (Berwanger et al., 2002). The chips used in the present study contained 11,800 clones from the human sequence-verified UniGene cDNA sets gf200, gf201 and gf202 (<http://www.resgen.com>). Cells at 4 h after irradiation were selected as treated samples and compared with unirradiated cells as well as a combination of unirradiated cells, carbon ion (2 Gy) and X-ray (6 Gy) irradiated cells. In order to balance the different intensities between these two dyes, each experiment was performed as sandwich hybridization including reverse labeling with Cy5 and Cy3 dye for a second microarray. This provides a replicated measurement for each hybridization, which can be used for quality control and for reduction of technical variability.

Microarrays were prehybridized for 30 min at 55 °C with a blocking solution containing 1% bovine serum albumin, 3 × SSC and 0.1% SDS. In order to reduce unspecific background signals, Cot1 DNA and polyA DNA were added to the labeled cDNA samples. The final volume of each sample loaded on the microarray chip was 100 µl,

including 10 μ l SSC (20 \times) and 4 μ l SDS (2%). Hybridized samples were boiled for 2 min immediately before sandwich hybridization. After incubation in a humid chamber at 55 $^{\circ}$ C for 16 h, microarray chips were separated again and washed four times including twice with 0.13 SSC/0.1% SDS and twice with 0.13 SSC. Finally, the chips were washed in water and dried by centrifugation.

Microarray chips were scanned separately using a GMS 418 microarray scanner (MWG Biotech, Ebersberg, Germany). Red and green lasers were operated at 633 nm and 543 nm to excite Cy5 and Cy3, respectively. The fluorescent data were normalized and analysed to calculate relative expression levels of each gene and to identify differentially expressed genes using the ImaGene 3.0 software (BioDiscovery Inc., Marina Del Rey, USA)

3.5. Quantification of genes expression using qRT-PCR

For calculation of relative expression of gene using $2^{-\Delta\Delta Ct}$ method, the amplification efficiencies of target and reference gene must be approximately equal (Livak et al., 2001). Standard curves were constructed using serial dilutions of cDNA (input volume: 0.5, 1, 2 and 2.5 μ l) for selected differentially expressed genes and GAPDH.

To validate the microarray data, qRT-PCR was performed in an iCycler (Bio-rad, USA) using Absolute SYBR Green Mixes (ABgene, Germany). The primers used of selected differentially expressed genes were summarized in Table 1. The qRT-PCR reaction mixture contained 5 μ l of diluted cDNA, 1.0 unit Tag-DNA polymerase, 1.5 mM $MgCl_2$, 0.2 mM of each dNTP, and 5 pmol of each primer with a 25 μ l final volume. PCR reaction conditions consisted of pre-heat of 15 min at 95 $^{\circ}$ C, following by 30 s at 95 $^{\circ}$ C, 30 s at anneal temperature and 45 s at 72 $^{\circ}$ C for 40 cycles post initial 30 s denaturation at 95 $^{\circ}$ C, and a final extension for 2 min at 72 $^{\circ}$ C. The qRT-PCR was performed in triplicates and included a no-template sample as a negative control. The reaction was evaluated by melting curve analysis after the final cycle within the range from 58-95 $^{\circ}$ C. Relative quantification of gene expression was calculated using the $2^{-\Delta\Delta Ct}$ method (Livak et al., 2001). The mean Ct values from triplicate measurements were normalized to GAPDH used as internal control.

3.6. Functional analysis of differentially expressed genes using Faltigo plus and IPA

The annotation and functional classification of differentially expressed genes were performed by using the FatiGO plus web tool as well as the Ingenuity Pathway Analysis (IPA) software (Ingenuity Systems, Mountain View, CA) based on the Gene Ontology database and the Kyoto Encyclopedia of Genes and Genomes (KEGG) pathways (Kanehisa, 2002, Al-Shahrour et al., 2007). The IPA classified the genes based on different parameters including location, molecular and biological functions, and cellular components. Additionally, the identified genes were categorized and mapped to genetic networks and signaling, metabolic and functional pathways, and ranked to determine their significance. The score reflects the probability that a collection of genes equal to or greater than the number in a network could be achieved by chance alone. According to the suggestion of IPA software, a cut-off score value of 3 was set in this present study. This score value had a 99.9% confidence level and was considered significant.

3.7. Statistical analysis

The association between the transcriptional expression of irradiated and unirradiated cells was analysed using the Students t-test with the SPSS version 15.0 software (SPSS Inc., Chicago, IL). The Fisher's test was used to analyse the significance of canonical pathways and genetic networks identified by the IPA tool. A $p < 0.05$ was considered significant.

4. Results

4.1. Measurement of RBE of A549 cells

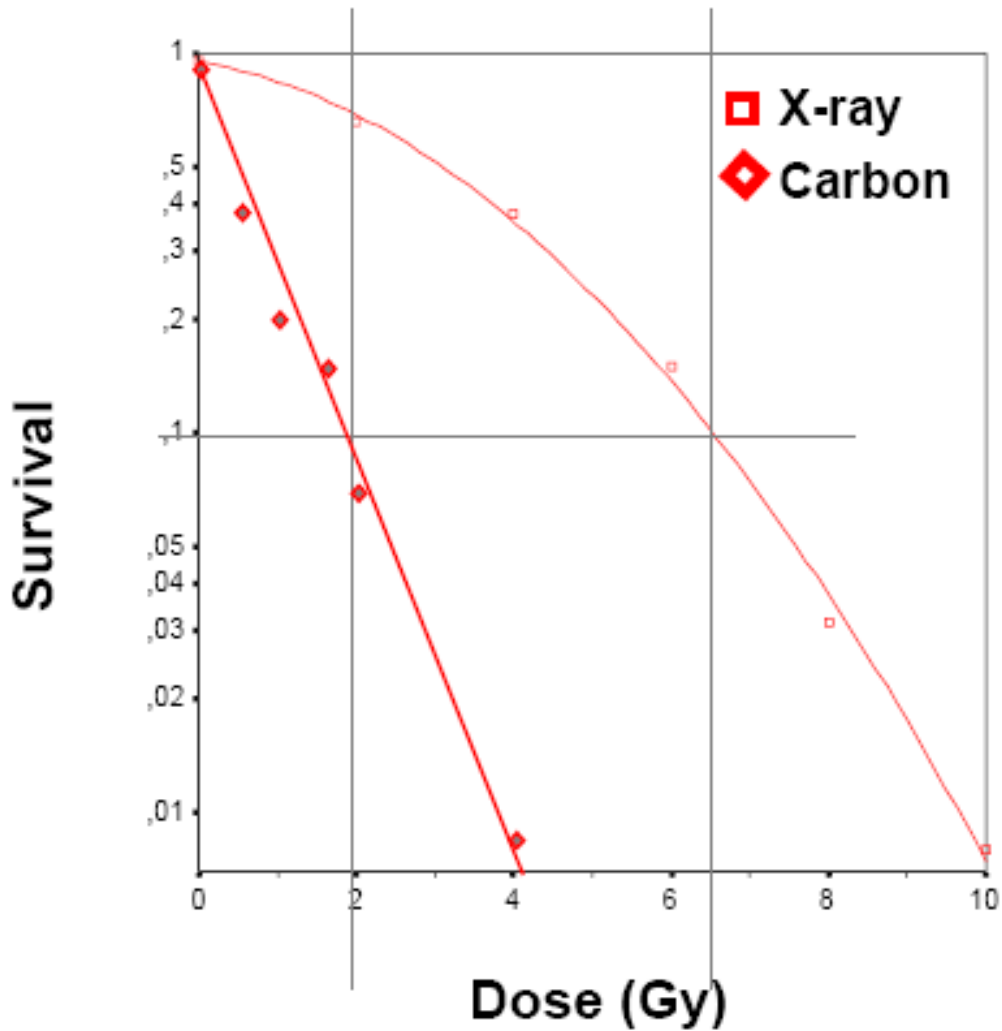


Fig. 7. Survival curves of A549 cells after irradiation with carbon ion and X-ray. X-axis showed the equivalent doses of carbon ion beam and X-ray. Y-axis went with the exponent survival rate of A549 cells. Squares represented the experiment points of cells irradiated with X-ray, as diamonds represented experiment points of cells irradiated with carbon ion beam. When at the 10% survival rate, the doses for carbon ion beam and X-ray were 2 Gy and 6 Gy, respectively.

In order to determine the biological equivalent dose between carbon ions and X-ray used in this study, colony forming assay was performed for the A549 cells after exposure to carbon beam and X-ray with different doses (Fig. 7). Carbon ions irradiation is slightly more effective than X-ray. According to the definition of RBE, the RBE10 with a survival fraction of 10% was approximately 3 with highly energy carbon ions. We therefore used 1/3 the physical doses of X-ray (6 Gy) for doses of carbon ion beams (2 Gy) in further microarray analysis.

4.2. RNA quality control

Because purity and integrity of RNA can have a tremendous affect on downstream analyses that from reverse transcription and microarray analysis to data interpretation of gene expression profiling, the control of RNA quality is of great importance. The purity and yield of RNA extracted from A549 cells were routinely determined using UV-spectrophotometer. Moreover, the integrity of RNA isolated was assessed by agarose gel electrophoresis to check for genomic DNA. As shown in Fig. 8, sharp and clear 28S and 18S rRNA bands are displayed in RNA samples analysed. The band of 28S rRNA appeared to be approximately twice as intense as 18S rRNA, indicating that the RNA samples were intact and remained to be mostly full-length.

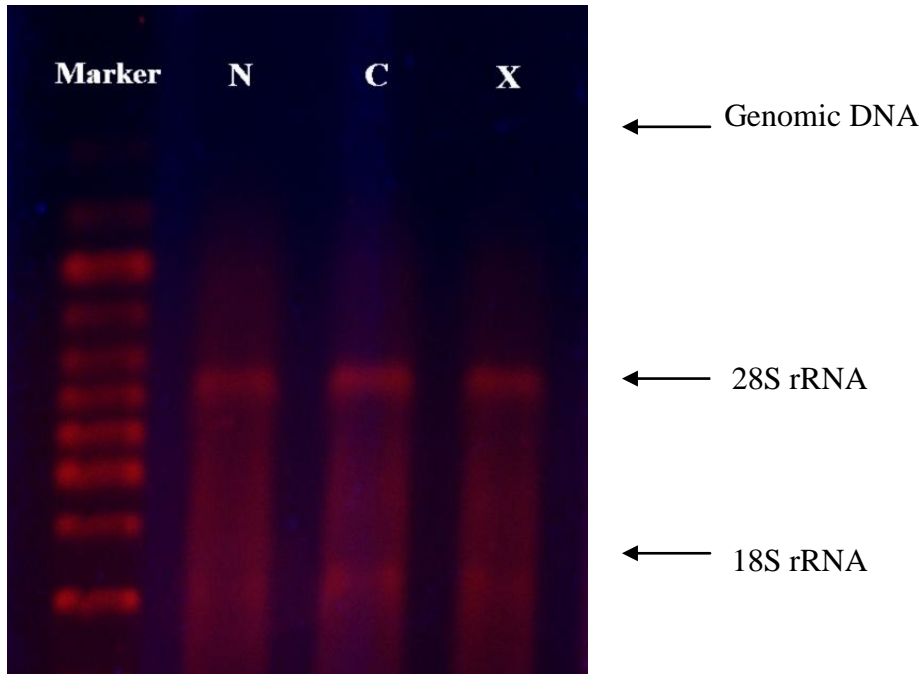


Fig. 8. Quality control of RNA by agarose gel electrophoresis. Total RNA was isolated from A549 cells and separated on a 1% agarose gel containing 0.5 % ethidium bromide. The 18S and 28S rRNA bands were clearly visible. N, non-irradiated; C, 2 Gy carbon ion irradiated; X, 6 Gy X-ray irradiated.

4.3. Pre-processing step of microarray data analysis

To examine the quality of microarray experiments, scatter plots of signal intensities were generated. For each spot, median signals and background intensities were obtained for both channels. The relationship between replicates of different samples was marked as a high degree of scatter and was not linear, indicating the microarray hybridizations were successful and could provide reliable data for further data analysis.

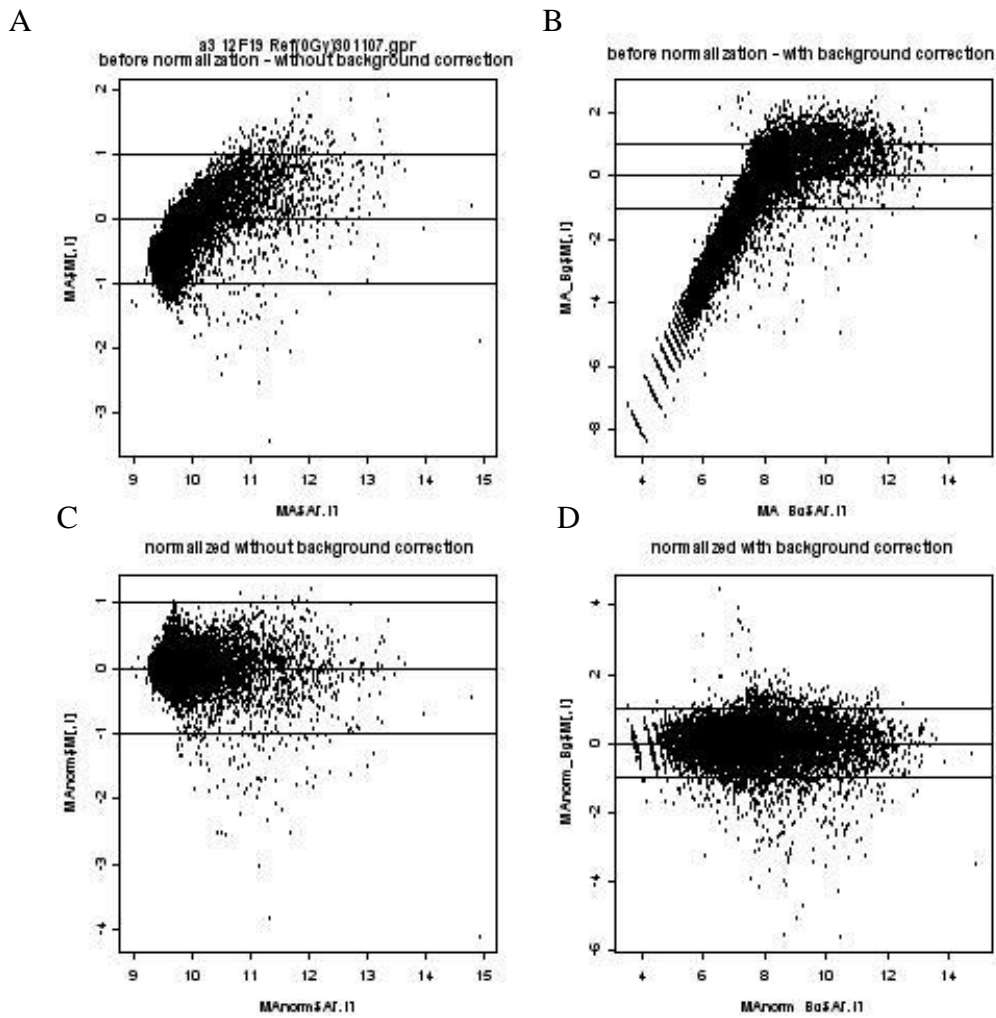


Fig.9. Scatter plots of median signal intensities of microarray data obtained from two channels. A showed signal intensities before normalized and without background correction. B showed signal intensities before normalized and with background correction. C showed normalized signal intensities without background correction. D showed normalized signal intensities with background correction.

4.4. Identification of genes regulated significantly by carbon ion beam radiation

The gene expression profiles of A549 cells at 4 h after carbon ion (2 Gy) and X-ray (6 Gy) irradiation were investigated using the cDNA microarray containing 11,800 gene transcripts. For each gene, the change in expression was calculated after carbon ion or, X-ray irradiation, as compared with control unirradiated cells by using the ImaGene 3.0 software.

Among the total of 11,800 gene transcripts, microarray analysis revealed a significant alterations (at least 2-fold) in the expression of 49 genes after 2 Gy carbon ion irradiation compared with control cells, and not affected by X-rays. Of these differentially expressed genes, 29 and 20 genes were up- and down-regulated, respectively.

To identify differentially expressed genes induced between irradiation with carbon ion and X-ray, the expression profiles of A549 cells exposed to carbon ion and X-ray were compared. The results of microarray analysis revealed that the expression levels of 326 genes were altered significantly (at least 2-fold) by carbon ion compared with X-rays. Among these genes identified, 169 were more up-regulated and 157 were down-regulated after carbon ion irradiation, than X-rays.

4.5. Gene networks and gene ontology analyses

4.5.1. Cellular functional classification of differently regulated genes

To determine the biological relevance of these differentially expressed genes, the cellular functional classification of these genes were analysed using the IPA software.

4.5.2. Genetic network and cellular functional classification of differentially regulated genes induced by carbon ion irradiation

In total, all of the 49 differentially expressed genes induced by carbon ions were mapped, and classified into genetic networks. The IPA tool delineated the involvement of 43 genes in 4 merged networks associated with important cellular functions (Fig. 10). Different molecular functions directly relevant to cancer signaling were identified i.e. cell cycle, cancer and cell death signaling (Table 2). Gene ontology analysis detected the canonical pathways with known implication in cancer (Table 3). Of these, statistically significant pathways such as aryl hydrocarbon receptor (AhR) signaling ($p = 0.007$) and G1/S cell cycle ($p = 0.012$) were identified. From these genes detected, CCND2, RARG and E2F5 were involved in both pathways.

Table 2 Merged genetic networks identified in A549 cells irradiated with carbon ions.

Network	Gene	Function	Score*
1	Calmodulin, <u>CAMK1D</u> , CASP8AP2, <u>CCND2</u> , <u>CD70</u> , FAS, <u>DDB2</u> , FAIM, FGF13, <u>GAP43</u> , <u>HBEGF</u> , IL31, Interferon alpha, Jnk, KIF11, LGALS7, MAPK, NCOA7, NFkB, NRIP2, NUAK2, P38 MAPK, PI3K, PKMYT1, <u>PPM1D</u> , PSMC3IP, <u>RARG</u> , <u>RIPK4</u> , RNA polymerase II, <u>SH2B1</u> , <u>THRB</u> , <u>TIMP3</u> , <u>TRIM32</u>	Cell Cycle, Hematological Disease, Gastrointestinal Disease	32
2	ARID1B, beta-estradiol, <u>BTBD10</u> , BUB1, <u>C11ORF51</u> , CDC25C, CDKN1A, CKS2, CKS1B, CRADD, <u>DCTPP1</u> , <u>DHPS</u> , E2F4, <u>E2F5</u> , EDN1, GHRHR, GTF2H4, KLK4, MIR292, MIR106A, MIRLET7B, MYC, NIF3L1, <u>NPHP4</u> , PCNA, <u>PCTK3</u> , PKMYT1, <u>PLEKHG3</u> , <u>POLS</u> , <u>PSAP</u> , TFDP3, TYMS, UBE2C, UNG, ZBED1	Cell Cycle, Cell Signaling, Connective Tissue Development and Function	19
3	ABL1, <u>APBA2</u> , CDC42, <u>CDC42BPA</u> , CDC42BPB, <u>CDC42EP1</u> , CKS2, Cofilin, <u>CTBS</u> , EGF, ERBB, FLII, GRB2, HIST1H1B, <u>HNRNPR</u> , HRAS, hydrogen peroxide, IL5RA, LGALS7, LIMK2, MAPKAP1, MYC, NCKIPSD, <u>OAZ2</u> , <u>PHKA2</u> , PLK3, PVR, RCC1, RELA, RPL26, <u>RPL21</u> , RPL7A, <u>SNRPG</u> , <u>Timp</u> , UBE2C	Cell Cycle, Cancer, Cell Death	17

4 B3GAT3, BRE, CD70, CDC14B, CTSD, Cell Death, 19
FAM179B, FAM40A, FGFR1OP2, HIC2, Amino Acid
HTT, KCNH2, MIRN326, PDCD10, PDK2, Metabolism,
PLK3, PPHLN1, PPL, PPME1, PPP1R3C, Molecular
PPP2R1A, PPP2R2A, RP6-213H19.1, SFXN3, Transport
SIK1, SIKE1, STK24, STK25, STRN, STRN3,
TAX1BP1, THRSP, TNF, TP53, TRAF3IP3,
UBQLN2

Network-eligible, overlapping genes (n=43) whose expression was modified after carbon ion irradiation but not by X-rays have been underlined. The rest of the genes either did not show any significant change or were not detected from the array; *A score>3 was significant.

Table 3 Canonical pathways in carbon ion-irradiated genes.

Ingenuity Canonical Pathways	p-value
Aryl Hydrocarbon Receptor Signaling	0.007762
Cell Cycle: G1/S Checkpoint Regulation	0.012589
p53 Signaling	0.030903
Glioma Signaling	0.033884
Pancreatic Adenocarcinoma Signaling	0.038019
Hereditary Breast Cancer Signaling	0.048978
Lipid Antigen Presentation by CD1	0.049234

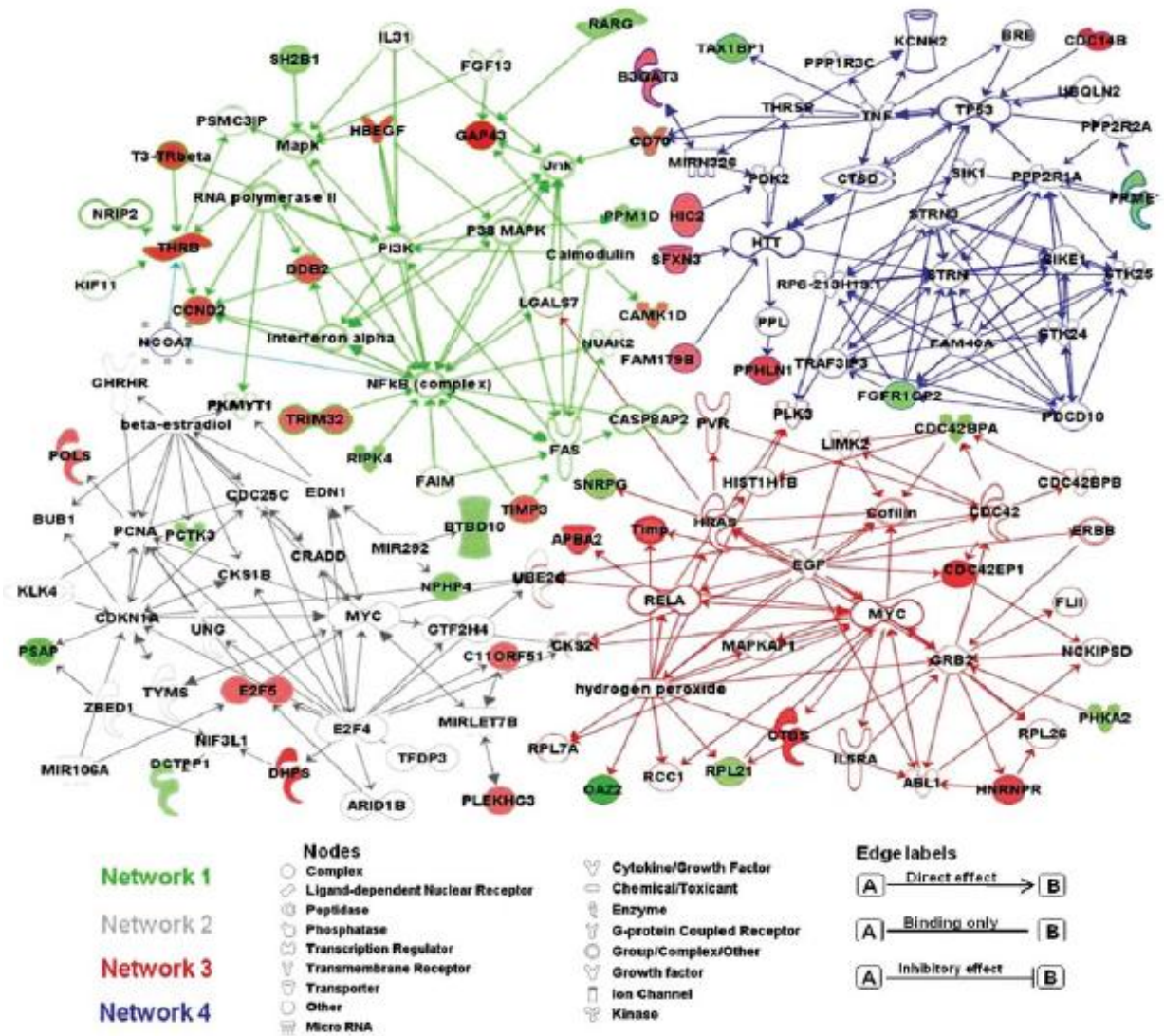


Fig.10. Interrelated networks of genes whose expression was modified after carbon ion irradiation. In total, four important networks of interrelated genes were identified. The four networks (green, network 1; orange, network 2; red, network 3; blue, network 4) were merged by overlapping genes (in bold). The degree of either up-regulation (red) or down-regulation (green) was reflected from the intensity of node color.

4.5.3. Genetic network of the up- and down-regulated genes between carbon ion and X-ray irradiation.

The gene expressions varied quite differently after different irradiations. The differences between the numbers of genes down- or up-regulated after exposure to both irradiations were highly significant in several pathways, with p values (FDR of < 0.05).

The functional analysis of the more up-regulated genes induced by carbon ion than X-ray determined three important functional networks involved in cellular growth and proliferation, cell cycle regulation, and oxidation reduction (Fig.11A-C). Of these 169 up-regulated genes, 152 network- and functional pathway-eligible genes were mapped and classified into genetic networks as well as pathways (Table 4). Among the more down-regulated genes after carbon ion, the functional analysis identified three important molecular functional networks associated with cellular function and maintenance of cancer, regulation of cell cycle in the DNA repair and recombination, and post translation modification (Fig. 12A-C). Of these 157 down-regulated genes, 145 network- and functional pathways-eligible genes were mapped and could be classified into functional pathways identified (Table 5). Among the transcripts significantly changed between carbon ion and X-ray irradiation, a number of genes was previously known to be radiation inducible, and another set of genes was newly identified as radiation regulated and was integrated in these functional networks. Several genes were involved in oxidation reduction (GLRX, NXN and RRM2) as well as in regulation of cell cycle and DNA damage response (CCND2, CDCA5, and CDC14B) were increased by carbon ion treatment. In contrast, a number of transcriptional regulators (BAI3, SIP1 and SP100) was significantly decreased by carbon ion than X-ray irradiation.

Of the molecular biological processes of these differentially expressed genes, top significant canonical pathways involved in important molecular functions response to DNA damages were identified (Table 6).

After carbon ion beam irradiation, expression of up-regulated genes fell mostly into the four top canonical pathways: G2/M damage checkpoint regulation, Hedgehog signaling, G1/S damage checkpoint regulation, and, oxidative phosphorylation, which indicated the activation of DNA damage checkpoint mechanisms of individual cells stopped acting as part of the whole organism and focused on self repair in cells after carbon ion beam irradiation. The top significant canonical pathways of the more down-regulated

genes by carbon ion irradiation than X-ray were involved in polyamine regulation in cancer, VDR/RXR activation, negative regulation of cell proliferation, and cyclin in cell cycle regulation which indicated that carbon ion beams provoke cell cycle arrest and inhibit cell proliferation (Table 6).

Table 4. Genetic networks of up-regulated genes between carbon ion and X-ray.

Network	Gene	Function	Score*
1	<u>AURKA</u> , <u>AURKB</u> , <u>BIRC5</u> , <u>CCNB1</u> , <u>CCND2</u> , <u>CDC6</u> , <u>CDK1</u> , CDKN1A, CHFR, Cyclin A, <u>CYFIP2</u> , DOT1L, <u>EED</u> , <u>ELAVL1</u> , <u>EPC1</u> , <u>EZH2</u> , <u>FEN1</u> , Histone h3, Histone h4, <u>HSPH1</u> , <u>ILF3</u> , <u>KCNA1</u> , <u>LMNB2</u> , <u>MYC</u> , <u>NCOA3</u> , <u>PNN</u> , <u>PTBP1</u> , PTMA, <u>PTRF</u> , RNA polymerase II, RPL10A, <u>RRM2</u> , <u>SMAD4</u> , THRAP3, <u>TOP2A</u>	Cellular growth and proliferation, Cellular movement	40
2	AKAP12, BIK, BTG1, CDC14A, <u>CDC14B</u> , CDT1, CEBPA, CENPE, <u>CENPF</u> , CSTF1, <u>CUL4A</u> , DUT, E2F4, <u>EIF2C2</u> , <u>FAS</u> , GBP1, <u>H2AFX</u> , <u>HIPK2</u> , <u>HMGB3</u> , ISG15, KLF5, <u>MAD2L1</u> , MCM6, MLH1, <u>MPO</u> , NEK2, <u>PLK1</u> , <u>POLA2</u> , <u>PPM1D</u> , PPP1R13B, PPP2R2B, RFC3, RNR, TP53, <u>YLPM1</u>	Cell cycle regulation DNA Replication Recombination and Repair	16
3	ARHGEF5, BTG, CBY1, CEBPA, <u>COX10</u> , CRADD, CTNNB1, DUSP4, DUT, E2F1, <u>GLRX</u> , KLF4, MAP3K5, <u>MPO</u> , NEDD8, <u>NXN</u> , <u>OAZ2</u> , <u>ODC1</u> , PPP1R13B, PTGS2, RAD23A, RFC3, <u>RRM2</u> , SOD2, TMSB15A, TP53, TRD, <u>YWHAH</u> , <u>YWHAZ</u>	Oxidation reduction	9

Network-eligible, overlapping genes (n=152) whose expression was more up-regulated after carbon ion irradiation than X-rays have been underlined. The rest of the genes either did not show any significant change or were not detected from the array; *A score>3 was significant.

Table 5. Genetic networks of down-regulated genes between carbon ion and X-ray

Network	Gene	Function	Score*
1	<u>APOH</u> , <u>AQP3</u> , AURKA, <u>AURKAIP1</u> , CTNNB1, <u>CYB5A</u> , <u>GNAO1</u> , HAS2, HNF1A, HOXA5, <u>HSD17B8</u> , <u>ISG15</u> , KDM5B, LGALS3, <u>LGALS3BP</u> , MT1X, <u>RARB</u> , <u>RARG</u> , RXRA, <u>SAT1</u> , <u>SCNN1A</u> , TFRC, THBD, TP53, <u>TSPAN7</u>	Cellular function and maintenance Cancer	18
2	BCL2L11, BMP4, <u>CCL2</u> , CCNA2, CCND3, CCNE2, CCNT1, CDK6, CDKN1B, CDKN2C, CEBPD, COPS5, DBF4, E2F1, FAS, <u>GABPA</u> , <u>GLRX</u> , GNAI2, <u>GPX2</u> , HIST4H4, HLTf, IFNGR1, IGF1, IGF1R, IGFBP3, MAP3K5, MYCN, <u>OAZ2</u> , SKP2, SOCS2, SP1, <u>TOB1</u> , TP63, ZNF217, <u>ZNF616</u>	Cell cycle, Cell death, Recombination and repair	12
3	APH1A, APH1B, <u>BAI3</u> , BLM, CCNE2, CDKN1A, CSTF1, <u>CXCL1</u> , DDB2, DHX9, <u>DIO2</u> , DUT, E2F4, H2AFX, <u>HIST2H2BE</u> , HOXA5, JUN, MCM6, <u>NCSTN</u> , NEK2, <u>PLSCR1</u> , PPP1R13B, PSEN2, PSENNEN, RFC3, RFW2, Secretase gamma, <u>SIP1</u> , <u>SOD2</u> , <u>SP100</u> , STMN1, TOPBP1, TP53, TTK, <u>WHSC2</u>	Post translation modification, Cell cycle	11

Network-eligible, overlapping genes (n=145) whose expression was more down-regulated after carbon ion irradiation than X-rays have been underlined. The rest of the genes either did not show any significant change or were not detected from the array; *A score>3 was significant.

Table 6. Canonical pathways of the differentially expressed genes

Ingenuity Canonical Pathways	p-value
Upregulated genes	
Cell cycle G2/M checkpoint regulation	0.000016
Hedgehog Signaling	0.000105
Cell cycle G1/S checkpoint regulation	0.000175
Oxidative phosphorylation	0.000196
Down-regulated genes	
Polyamine regulation in cancer	0.000253
VDR/RXR activation	0.000261
Negative regulation of cell proliferation	0.000297
Cyclin in cell cycle regulation	0.000435

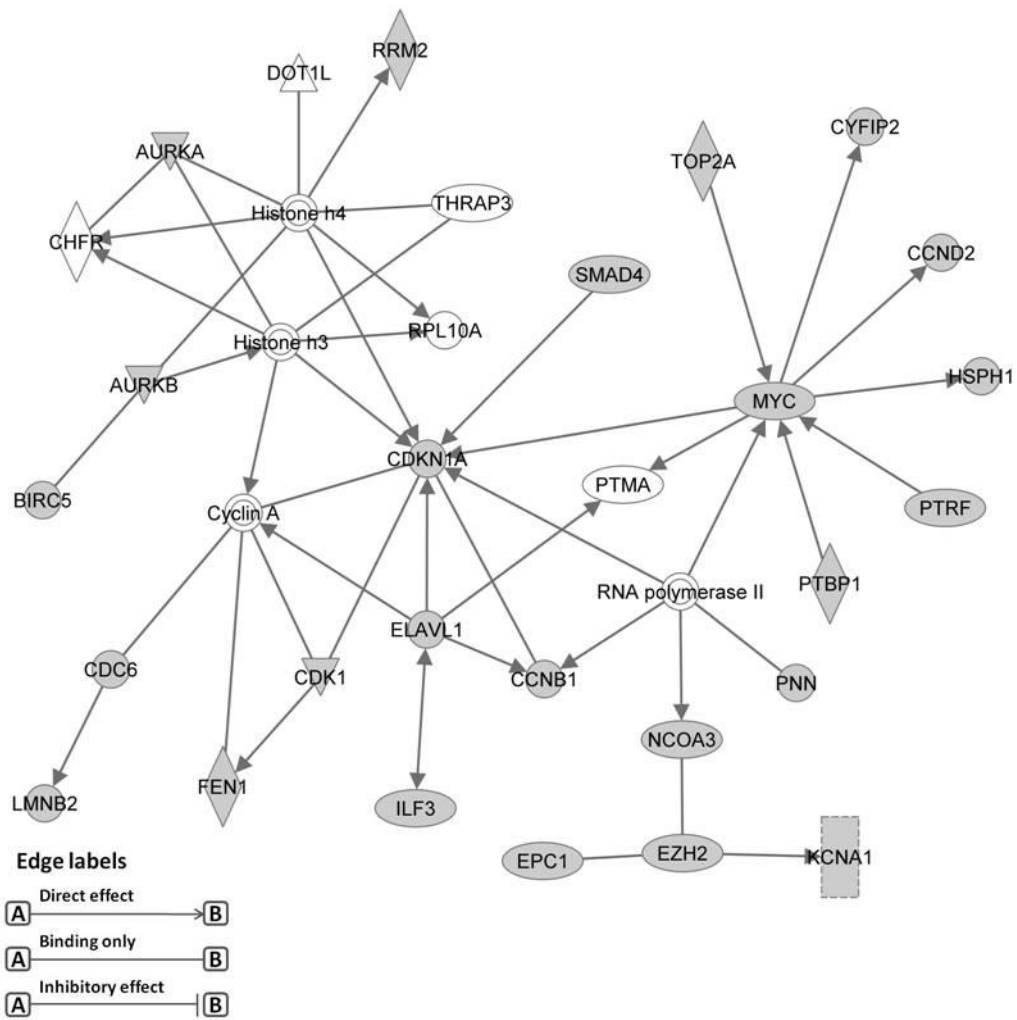


Fig.11A. Network 1 (cellular proliferation) of up-regulated genes between carbon ion and X-ray irradiation

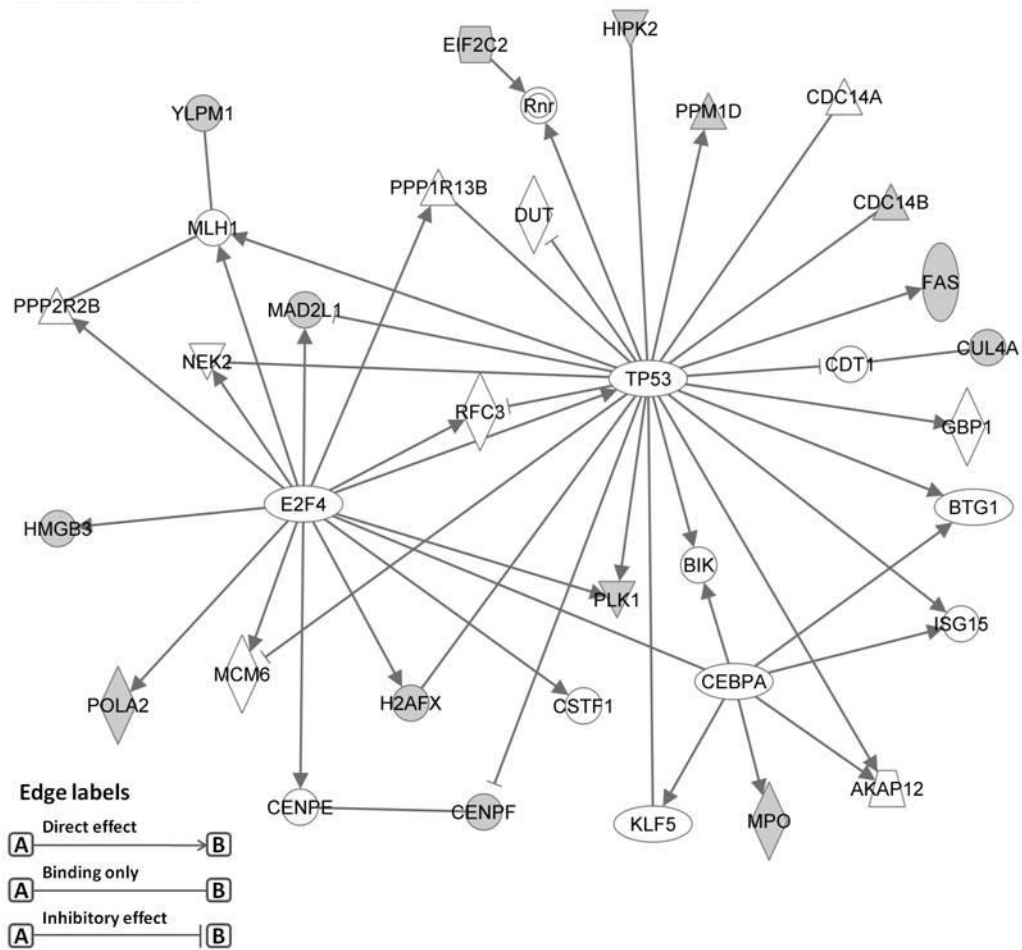


Fig.11B. Network 2 (cell cycle regulation) of up-regulated genes between carbon ion and X-ray irradiation

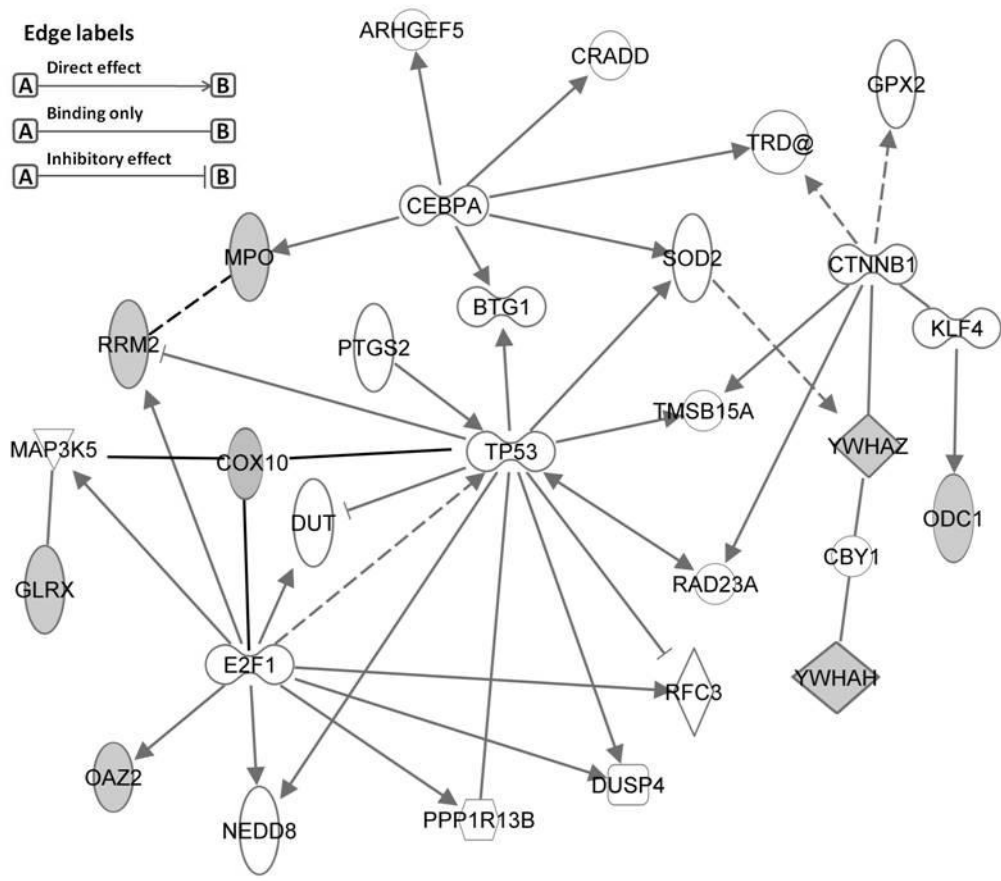


Fig.11C. Network 3 (oxidation reduction) of up-regulated genes between carbon ion and X-ray irradiation

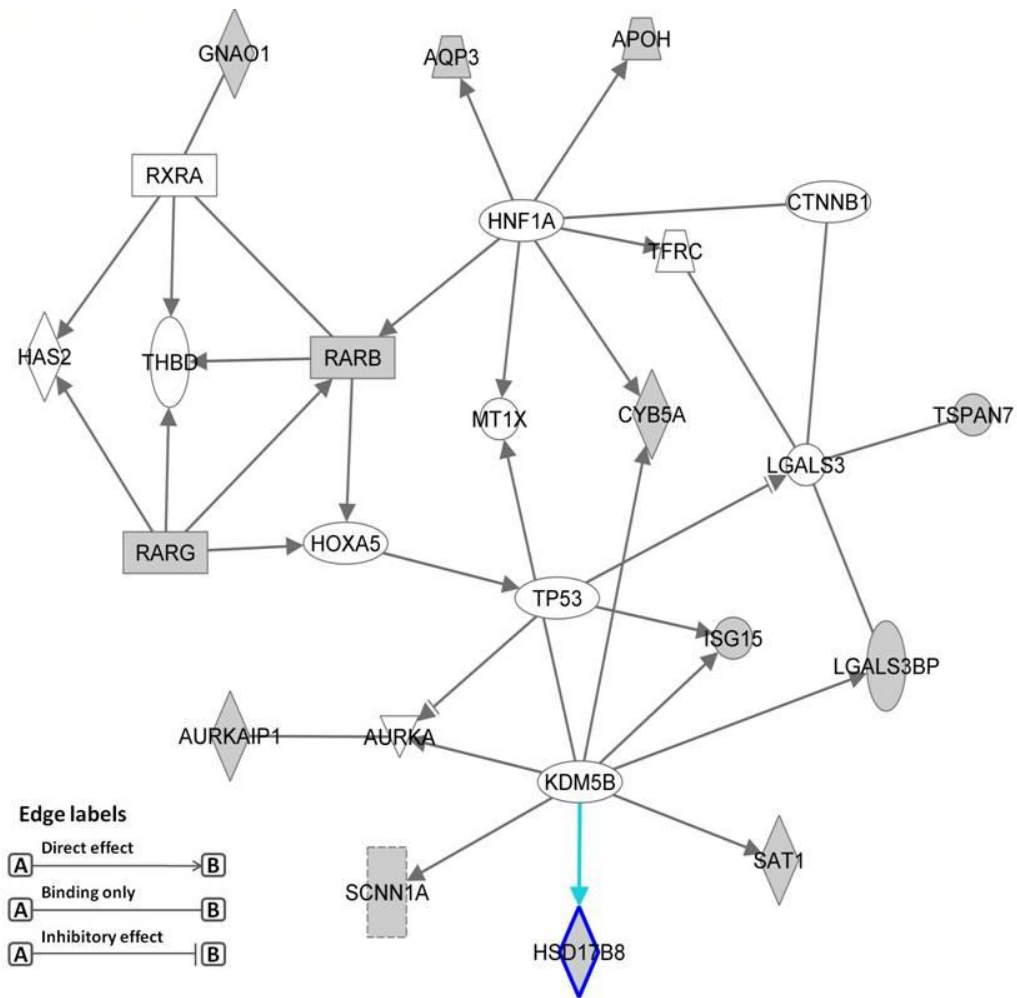


Fig.12A. Network 1 (cellular function and maintenance of cancer) of down-regulated genes between carbon ion and X-ray irradiation

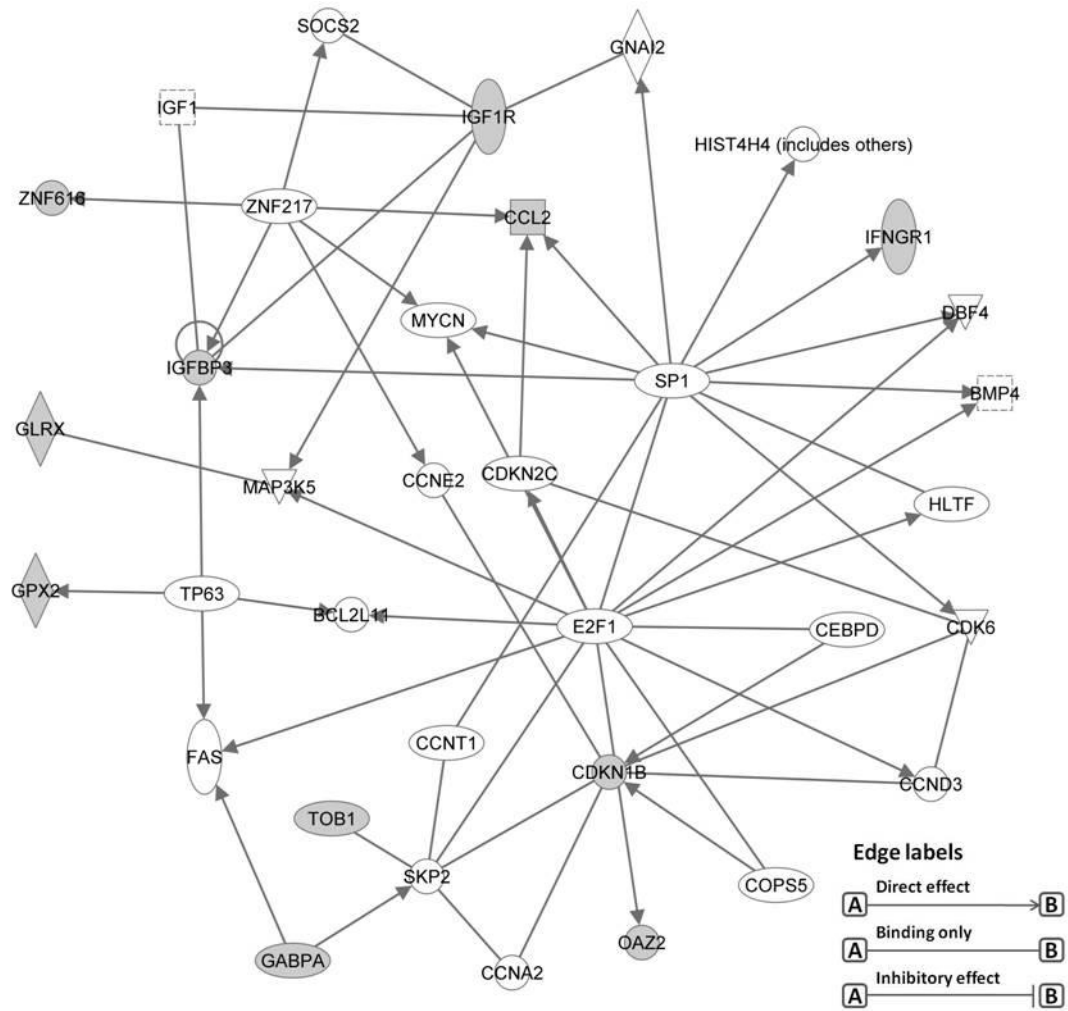


Fig.12B. Network 2 (cell cycle regulation) of down-regulated genes between carbon ion and X-ray irradiation

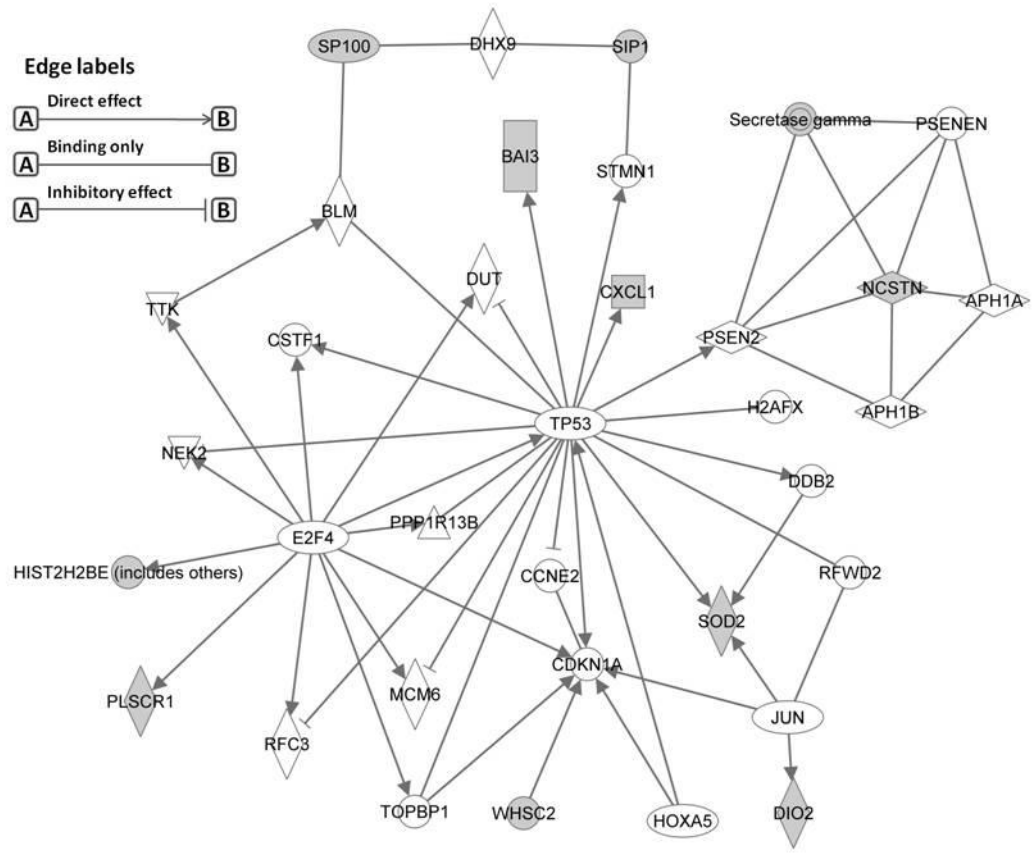


Fig.12C. Network 3 (post translation modification) of down-regulated genes between carbon ion and X-ray irradiation

4.6. Validations of the gene expression by qRT-PCR

4.6.1. Standard curves of primers used

One of the important factors for the employment of relative qRT-PCR to validate microarray results is that the PCR efficiencies of the housekeeping gene and the candidate genes should be close to identical. In the present study, GAPDH was chosen as the internal standard because its widely used in study of various cancers.

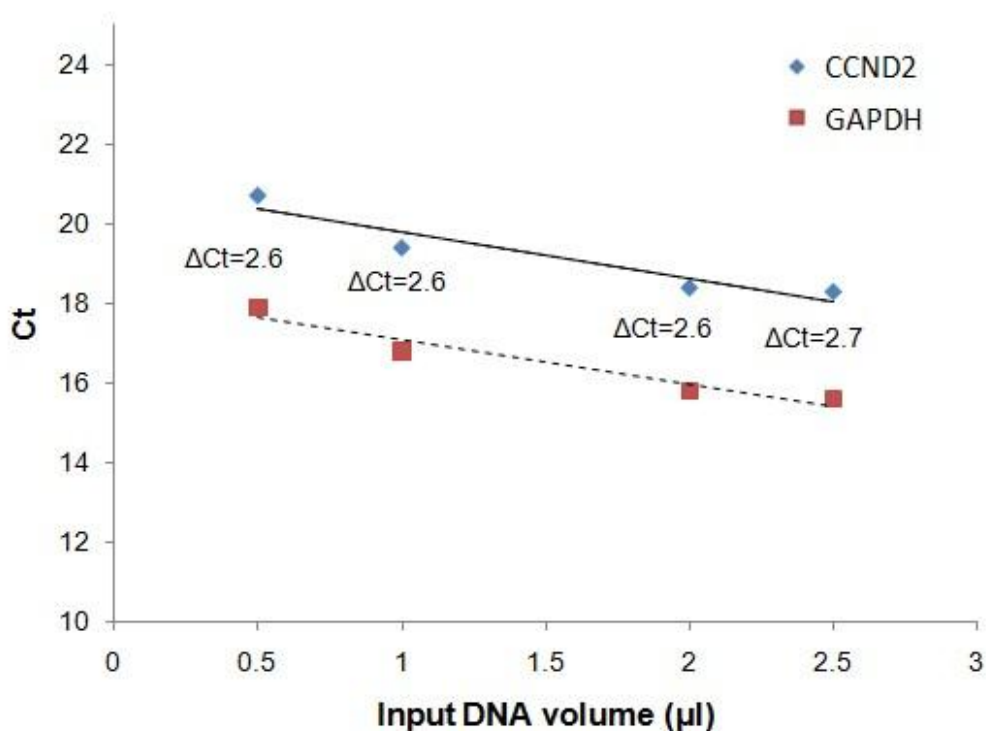


Fig.13. Determination and comparison of the qRT-PCR efficiencies of GAPDH and candidate (CCND2). The X-axis showed the input volume of DNA (cDNA synthesized directly from mRNA extracted from irradiated A549 cells, same as used in microarray analysis). Each point represented the mean of triplicates of reactions. Y-axis showed the corresponding Ct value of the DNA samples. Squares represent the experiment points of GAPDH, while diamonds represented for CCND2.

The efficiencies of qRT-PCR for selected candidate genes and reference gene GAPDH were determined using standard curves with series dilution of input templates.

Representative standard curve for amplification of CCND2 and GAPDH were illustrated in Fig. 13.

The straight side (dotted line) of the PCR of the referent gene GAPDH with a slope = -1.12 ($R^2 = 0.9368$). The straight side (continuous line) of the PCR of the CCND2 gene with a slope = -1.16 ($R^2 = 0.8995$). The Ct values increase had good linear relationship with the quantity of input DNA and showed paralleled between candidate gene CCND2 and GAPDH, suggesting similar efficiencies of amplification for both genes analysed. Under this premise, $2^{-\Delta\Delta C_t}$ method can be applied in the calculation of the relative expression of genes.

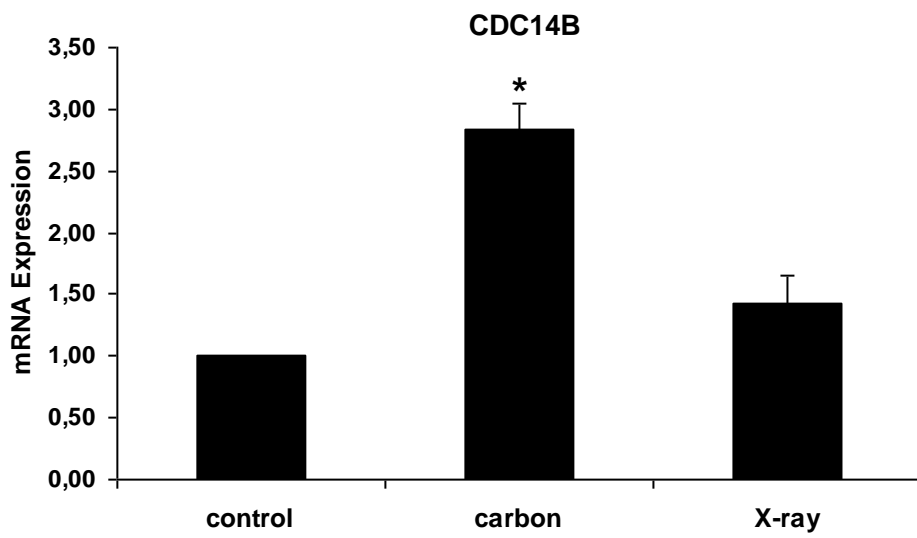
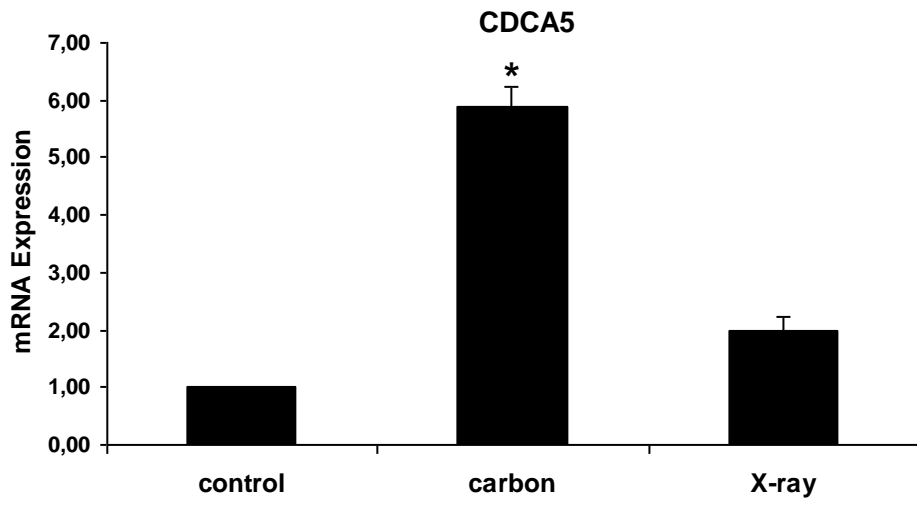
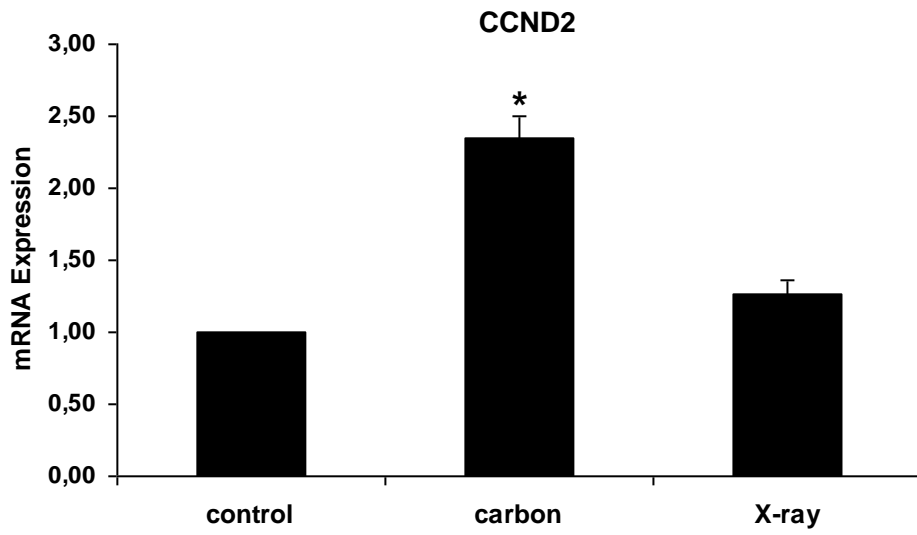
4.6.2. Expression levels of irradiated genes

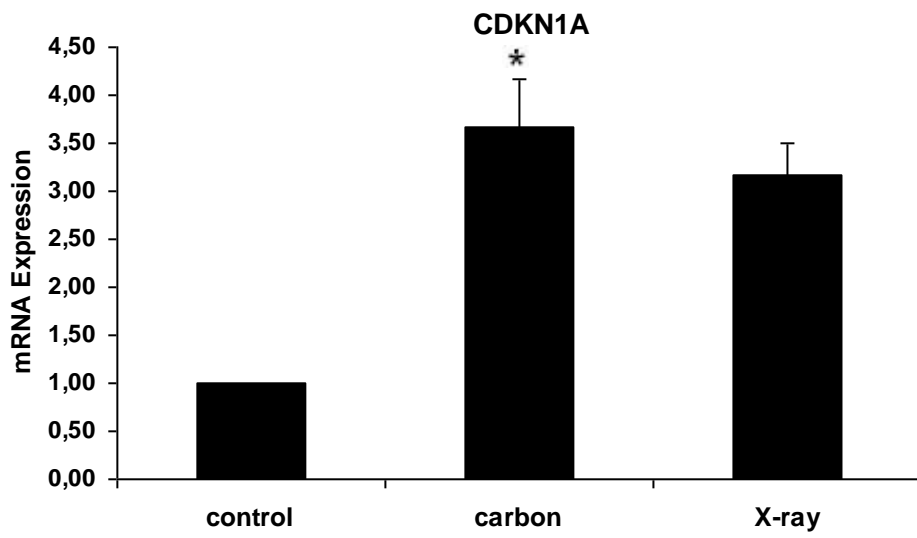
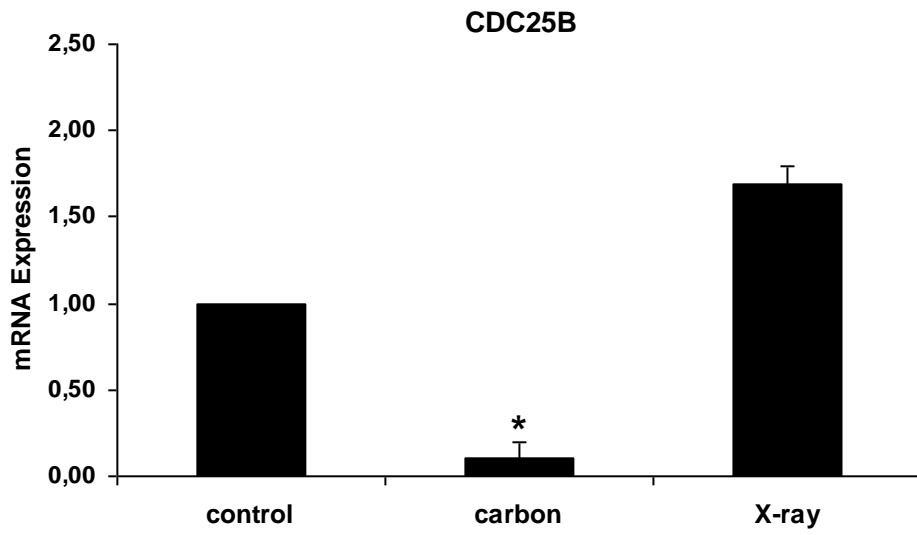
To validate the consistency and reproducibility of microarray experiments, a subset of 8 differentially expressed genes involved in cell cycle, DNA damage and transcription were analysed by qRT-PCR. The cellular functions of the selected genes are summarized in Table 7. Expression levels were normalized with the housekeeping gene GAPDH and calculated as fold change value of irradiated cell versus unirradiated control.

Among these 8 genes analysed, CDKN1A was up-regulated at 4 h by both irradiations with carbon ion and X-ray. Use of qRT-PCR analysis, we confirmed the up-regulation of cell cycle related genes CCND2, CDCA5, CDC14B, as well as E2F5, which are involved in promoting of transcription and proliferation of cell. Carbon ion irradiation showed significant effects on the expression of these 4 genes than X-ray. In contrast, the expression level of CDC25B, TP53I11 and RARG decreased more effectively after X-ray than carbon ion irradiation (Figure 14).

Table 7. Functions of genes selected for the validation of microarray results.

Gene symbol	Gene name	Function
CCND2	cyclin D2	cell cycle
CDCA5	cell division cycle associated 5	cell cycle
CDC14B	cell division cycle 14 homolog B	DNA damage, cell division
CDC25B	cell division cycle 25 homolog B	DNA damage, cell division
CDKN1A	cyclin-dependent kinase inhibitor 1A, p21	cell cycle, DNA damage
E2F5	transcription factor 5, p130-binding	transcription, proliferation
RARG	retinoic acid receptor, gamma	transcription
TP53I11	tumor protein p53 inducible protein 11	DNA damage, transcription





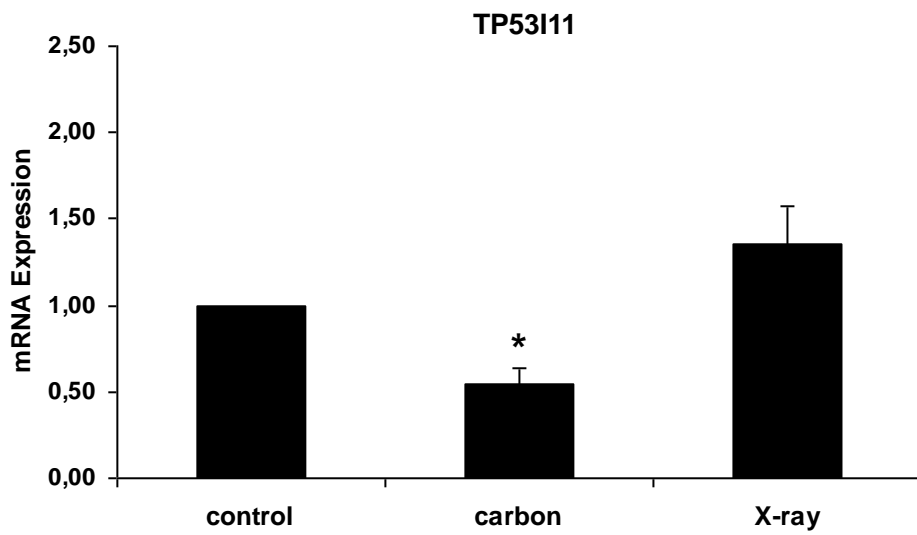
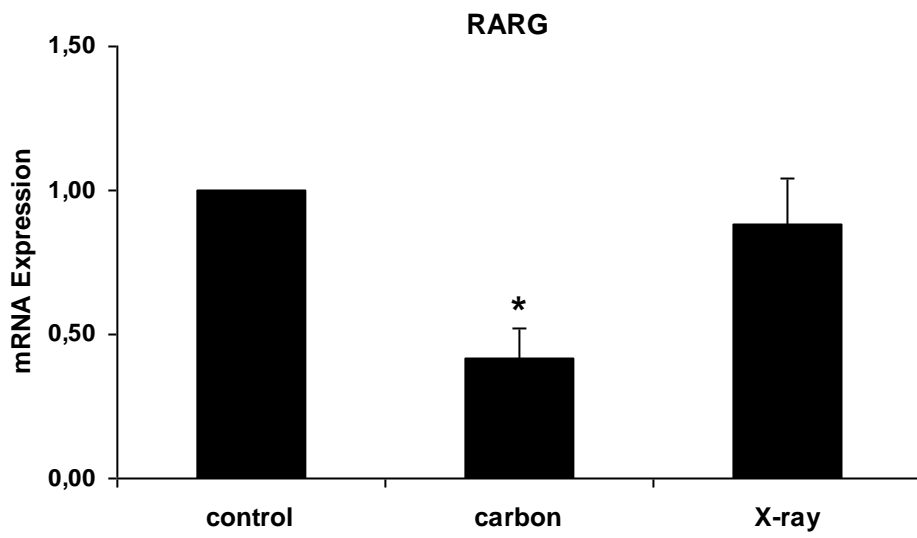
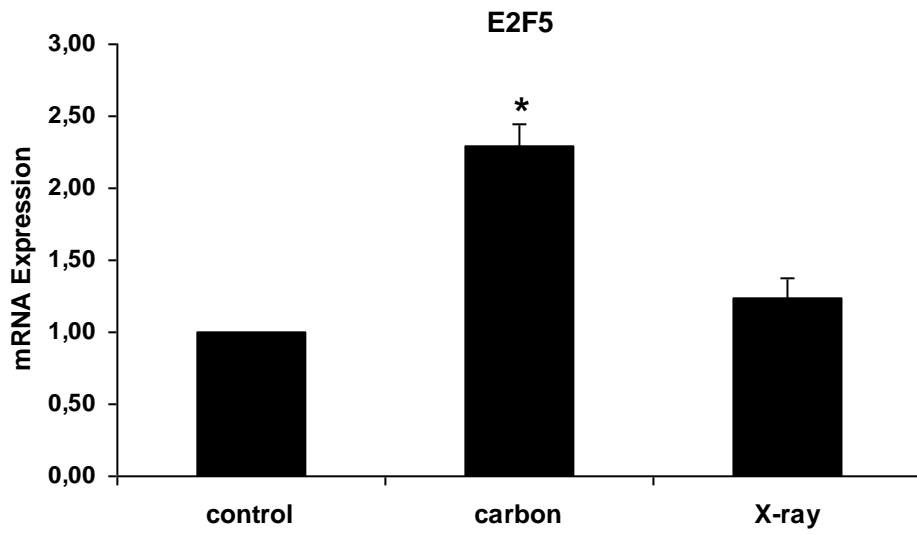


Fig.14. Validation of selected genes in A549 cells 4 h after carbon ion beam and X-ray irradiation using qRT-PCR. The qRT-PCR results of transcriptional expression were normalized to the values of GAPDH gene and then expressed as fold in comparison to unirradiated, control cells (0 Gy). Data were expressed as mean \pm SD. * $p < 0.05$ using Student's test for comparison between carbon ion and X-ray irradiation.

5. Discussion

In this study, the gene expression profiles were investigated in lung adenocarcinoma cell A549 after irradiation with carbon ion and X-ray. The differently expressed genes with their functional categories and biological pathways associated with carbon ion induced DNA-damages were analysed using web-based transcriptional networks. Changes in transcriptional expression of selected differently expressed genes involved in important cellular functions response to DNA damages were assessed by qRT-PCR. The identification of different expression changes suggested different effects on gene expressions between carbon ions and X-ray and might contribute to a better understanding of the molecular response to carbon ion irradiation in lung cancer cells.

5.1. Increased RBE of carbon ion on A549 cells

Due to its superior physical and biological characterizations, heavy ion beams can induce highly complex clustered DNA damages resulting in increased biologic effects (Hamada, 2009). Previous experimental data demonstrated that heavy ions including carbon ion are more effective on cell killing than X-ray (Cox et al., 1977, Goodhead et al. 1993). The increased RBE represents one of the major rationales for the application of heavy ions in tumor therapy. Blakely et al. (1979) reported that the RBE values of T-1 kidney cells were about 1.2 for 13-KeV/ μm and 2.3 for 85-KeV/ μm carbon beams. However, different types of ion beams with similar LET values resulted in different cell killing effects, indicating that biological effects caused by heavy ions strongly associated with the characters of ion beams (Fokas E et al., 2009). Following carbon ion (29 KeV/ μm) exposure, an enhanced frequency of apoptotic cells and an increase in aberrant cells were observed in human hematopoietic stem and progenitor cells, resulting in a RBE of 1.4-1.7 compared with X-ray (Becker et al., 2009). Suzuki et al. (2000) in Chiba, Japan have systematic analysed 14 tumor cell lines exposed to carbon ions with two different LET values. The reported RBE values were 1.06-1.33 for 13 KeV/ μm and 2.00-3.01 for 77 KeV/ μm carbon beams. These studies have provided the RBE values of many types of normal and carcinoma cells and suggested that the increased RBE associated with increasing LET values of ion beams (Suzuki et al., 2000; Sørensen et al., 2011). In the

present study, we assessed the RBE of A549 cells irradiated with high LET carbon beams (170 KeV/ μm), an energy of carbon ions routinely used in the GSI (Fournier et al., 2004). In line with previous report using carbon ions with lower LET values (13.3 and 77 KeV/ μm), an enhanced RBE value for high LET carbon beams was detected in present study, suggesting the LET dependence of cell killing effect.

5.2. Gene expression profiling changes differently between X-ray and carbon ion radiations

Experimental studies *in vitro* and *in vivo* demonstrated differences in the regulation of cell cycle, DNA repair, angiogenesis and apoptosis on normal epithelia and carcinoma cells between photon- and heavy ion irradiation. However, few studies have investigated genetic aberrations and gene expression induced by heavy ion irradiation. The molecular mechanisms and the signaling pathways involved in cellular responses to heavy ion radiation are not completely understood.

Kurpinski et al. (2009) compared the biological effects of ^{56}Fe ions and X-ray on human mesenchymal stem cells and found distinct differential transcriptional regulation associated with more significant effects of ^{56}Fe ions on DNA/RNA metabolism, cell cycle regulation and DNA-binding activity using an Affymetrix microarray containing 22,277 probe-sets. Using a cDNA expression array containing 161 genes of DNA damage and repair signaling pathway, Roy et al. (2008) examined the gene expression profiling of breast epithelial cell MCF-10F exposed to lower doses of ^{56}Fe ions and X-ray. Of the 161 genes analysed, 30 and 16 genes were altered by X-ray and ^{56}Fe ions, respectively. Two recent studies on OSCC in Chiba, Japan have showed that 98 genes were induced significantly by carbon ion irradiation at all dose points in the three OSCC cell lines compared with unirradiated control cells (Higo et al., 2006, Fushimi et al., 2008).

Moreover, Akino et al. (2009) have showed the effect of carbon ion beam on the aggressiveness and gene expression of A549 cell and identified 23 and 22 up- and down regulated genes after carbon ion irradiation using PCR technology. Although these studies analysed different cells exposed to different heavy ions with different LET, the observations in these studies as well as our results in this study demonstrated special changes in gene expression induced by heavy ions and provided preliminary

evidence linking alterations in global gene expression and changes in cellular responses after heavy ions irradiation.

5.3. Signaling pathways of different expressed genes between carbon ion irradiation and X-ray

The pathway analysis of the up-regulated genes between carbon ion and X-ray irradiation in this study have showed that mostly overrepresented biological processes of these genes were cell proliferation and oxidation reduction by using the IPA pathway tool. Tumor hypoxia is a well-recognized factor contributing to tumor progress, angiogenesis and genetic instability (Denko NC., 2008). Radiation generated reactive oxygen species lead to formation of DNA lesions such as DSBs and act as the principal determinants of cell killing (Dewhirst et al., 2008). However, high-LET irradiation induces clustered DNA damage that is much less dependent on the formation of reactive oxygen species for cell killing than X-ray, since OER decreases with increasing LET (Curtis et al., 1984). Several genes such as GLRX, NXN and RRM2, involved in the oxidation and reduction were found to be altered after carbon ions irradiation in this study. The enzyme glutaredoxin (GLRX) can inhibit NFkB survival pathway and promote apoptosis in hypoxic cancer cells (Qanungo et al., 2007). NXN is reactive oxygen species regulator involved in cell growth and differentiation. Expression of NRN can inhibit Wnt pathway and lead to promote apoptosis and enhance radiosensitization in cancer stem cells (Chen et al., 2007; Funato Y et al., 2008). The ribonucleotide reductase subunit RRM2 is essential for DNA synthesis. Activation of RRM2 by an ATR/ATM-CHK1-E2F1 pathway is implicated in the regulation of cell cycle and DNA repair after DNA damage (Zhang et al., 2009). Experimental data in vivo and clinical results have demonstrated that heavy ion therapy reduces hypoxia-driven tumor radioresistance (Furusawa et al., 2000). The enhanced induction of these genes involved in oxidation reduction and cell proliferation after carbon ion radiation in this study suggested that the activation of these pathways may be differently regulated between carbon ion and X-ray radiation.

Experimental findings from both synchronous and asynchronous cell populations have found that heavy ion irradiation induced more pronounced G1-phase and

prolonged G2/M-phase delay, which could account for the increased effectiveness of heavy ions compared with X-rays. (Scholz et al., 1994, Goto et al., 2002, Nasonova et al., 2004). Our functional network analysis revealed that the down regulated genes between carbon ion and X-ray irradiation were mainly involved in cell mitosis, cell cycles and division. Critical transitions in the different phases of the cell cycle are regulated by sequential activation of cyclins and their catalytic subunits, the cyclin-dependent kinases (Malumbres et al., 2009). In response to DNA damage such as irradiation, the suppression of CDKs and the activation of CDK inhibitors induce cell cycle delay or arrest to allow time for either the repair of DNA damage or the elimination of genetically unstable cells by apoptosis (Jeggo et al., 2006). In the present study, we found down-regulation of CDK1, CCNB1 and CDC25B and up-regulation of CDK inhibitor p21, are more responsible to carbon ions than X-ray. The CDK inhibitor p21 plays key roles in DNA-damage responses such as cell cycle checkpoints, senescence, and apoptosis (Abbas T and Dutta A, 2009). Precious studies on fibroblasts as well as cancer cells have found that heavy-ion traversal (calcium and carbon ions) formed p21 foci, that resembled extremely the pattern of charged particles and persisted for several hours, in contrast to X-rays where a short-lived, diffusely spread pattern was observed (Jacob et al., 2002; Fournier C et al., 2004; Koike et al., 2011). Irradiation with carbon ion with varying LET values (300 to 13600 KeV/ μm) revealed a strict spatial correlation for the occurrence of CDKN1A and PCNA with MRE11B clusters as well as of CDKN1A with gamma-H2AX signals (Jakob et al., 2003). These findings suggested that the alterations of these repair genes might lead to less efficient rejoining of G1 and G2 DNA breaks, less repair and subsequently higher numbers of residual breaks induced by high-LET irradiation with carbon ions. In line with these observations, the alterations in expression of cell cycle regulators in the present study may, at least in part contribute to prolonged cell cycles delay in heavy ion irradiated cells.

Although the introduction of microarray technology is a great-leap-forward development in genomic variations of various tumor subtypes both experimentally and clinically, their high price and limitation of inter-study comparability hampered their widespread application. Therefore, quantitative real time polymerase chain reaction (qRT-PCR), as the most sensitive technique currently available for detection and quantification of gene expression, become the most suitable and powerful

complement arrays for the conformation and validation of individual transcripts in larger sample cohorts.

Basic research from biophysics and radiobiology has led to new, promising perspectives in particle therapy. The significant differences in radiobiology of heavy ions beams from the conventional photon radiobiology should be further studied for the benefit of cancer patients. Additional functional studies of the differently expressed genes identified in this study may clarify and extend the importance of these genes in the regulation of DNA damage after carbon ion radiation in lung cancer cells.

6. Future prospects

Carbon ions irradiation provides both physical and biological advantages and is promising for the treatment of NSCLC regarding local control and overall survival. Carbon ions can cause clustered DNA damage and lead to induction of transcriptional programs and activation of DNA damage response pathways. Our data in this study show different expression profiles in lung cancer cells irradiated with carbon ions and X-ray using high-density cDNA microarray and identify a set of differentially expressed genes. The functional classification of these differentially expressed genes suggests the involvement in important signaling pathways such as the regulation of cell cycle, DNA repair and oxidation and reduction. Understanding the molecular mechanisms underlying cellular response of carbon ions will certainly have an impact on numerous field of radiation therapy. Future experiments are needed to examine the functions of these genes in detail and will provide insights into their role in lung cancer cells exposed to carbon ions.

7. Summary

Background

Lung cancer is the leading cause of cancer-related death in men and the third in women in Germany. Radiation therapy plays an important role in the multimodal treatment of lung cancer. Due to the excellent dose distribution and the higher relative biological effectiveness (RBE) in tumor, heavy ion therapy with carbon shows promising clinical results in different types of cancer. However, the genetic differences of radiation induced reactions in cancer between heavy ion beams and conventional photon beams are not fully understood. In the present study, we compared the gene expression profiles of A549 cells after heavy ion radiation or X-ray radiation using a DNA microarray chip containing 11,800 human genes and identified differentially expressed genes. A set of selected differentially expressed genes was validated with quantitative real-time polymerase chain reaction (qRT-PCR).

Materials/Methods

The lung carcinoma cell line A549 was irradiated with carbon ion beams (9,8 MeV/nucleon) and X-ray (250 kV) using different doses. The biologically equivalent doses for each radiation quality were determined by clonogenic survival assay. The transcriptional profiling was determined with a high density cDNA microarray containing 11.800 genes, and genetic network and gene ontology analysis was performed. The expression changes of selected genes were validated by qRT-PCR.

Results

Microarray analysis revealed a significant alteration in the expression of 49 genes (at least 2-fold) after carbon ion irradiation and not altered by X-rays, as compared with unirradiated control cells. Of these 49 differentially expressed genes identified, 29 and 20 genes were up- and down-regulated, respectively.

Moreover, the results of microarray analysis showed that the expression levels of 326 genes were altered significantly by carbon ion irradiation with biological equivalent dose to X-rays. Among these genes identified, 169 and 157 genes were more up-and down-regulated in carbon ion irradiation, as compared to X-rays.

The genetic network and functional classification of the 49 differentially expressed genes between carbon ions irradiation and control unirradiated cells revealed four merged networks which were associated with the regulation of cell cycle, cancer and cell death signaling and cell signaling.

The functional analysis of the up-regulated genes between carbon ion and X-ray determined three important functional networks involved in cellular growth and proliferation, cell cycle regulation, and oxidation reduction. Among the down-regulated genes, the functional analysis identified three important molecular functional networks associated with cellular function and maintenance of cancer, regulation of cell cycle in the DNA repair, and post translation modification. A set of 8 selected differentially expressed genes involved in cell cycle, DNA damage and transcription was analysed by qRT-PCR and confirmed the microarray data.

Conclusions

These results showed that these two types of radiations, although in the same biological relative doses, could induce significant gene expression in different levels in A549 cells. The functional classification of these differentially expressed genes revealed that carbon ions and X-ray irradiations have different effects on different signaling pathways through gene expression. The identification of differentially expressed gene in this study might add to the understanding of the complicated molecular responses to carbon ion irradiation and provided valuable resource for both experimental and clinical application of heavy ion beam for treatment of lung cancer.

7. Zusammenfassung

Das Lungenkarzinom ist die häufigste tödliche Krebserkrankung des Mannes und die dritthäufigste tödliche Krebserkrankung der Frau in Deutschland. Die Strahlentherapie spielt eine wichtige Rolle in der multimodalen Behandlung vom Lungenkarzinom. Aufgrund der hervorragenden Dosisverteilung und der höheren relativen biologischen Wirksamkeit (RBW) im Tumor zeigt die Schwerionentherapie mit Kohlenstoff vielversprechende klinische Ergebnisse bei unterschiedlichen Karzinomen. Die genetischen Unterschiede der Strahlenreaktionen im Krebsgewebe nach intensiver Ionenbestrahlung und konventioneller Photonenbestrahlung sind aber bis heute nicht vollständig geklärt. In der vorliegenden Arbeit wurden deshalb die Expressionsprofilen humaner A549 Lungenkarzinomzellen nach Bestrahlung mit Kohlenstoffionen und Röntgenstrahlen mittels eines cDNA Microarrays mit 11.800 menschlichen Genen verglichen und differentiell exprimierte Gene identifiziert. Mit quantitativer Real-Time PCR (qRT-PCR) wurden die Veränderungen der ausgewählten differentiell exprimierten Kandidatengene analysiert.

Die A549 Lungenkarzinomzellen wurden mit Kohlenstoffionen (9,8 MeV/nucleon) und Röntgen (250 kV) bestrahlt. Die biologischen Äquivalentdosen der Kohlenstoffionen und Röntgenstrahlen wurden mit dem klonogenen Überleben-Assay bestimmt.

Im Vergleich zur unbestrahlten Kontrolle zeigte die Mikroarray-Analyse signifikante Veränderungen der Expression von 49 Genen (mindestens 2-fach) nach Bestrahlung mit Kohlenstoff. Davon waren 29 Gene und 20 Gene hoch- und runterreguliert. Anhand der Analyse der Expressionsprofile konnten 326 differentiell exprimierte Gene zwischen Bestrahlung mit Kohlenstoffionen und Röntgenstrahlen mit den biologischen Äquivalentdosen identifiziert werden. Im Vergleich zur Röntgenstrahlung waren 169 bzw. 157 Gene nach Bestrahlung mit Kohlenstoffionen signifikanter hoch- und runterreguliert. Die genetische Netzwerk und funktionelle Klassifizierungen der 49 differentiell exprimierten Gene zwischen Kohlenstoffionenstrahlung und unbestrahlter Kontrolle zeigten vier fusionierten

Netzwerke, welche in der Regulation des Zellzykluses, des Zelltods, und des Zellsignalwegs beteiligt sind. Weitere funktionelle Analyse der hochregulierten Gene zwischen Kohlenstoffionen und Röntgenstrahlen zeigte drei wichtige funktionelle Netzwerke, welche an der Regulation der zellulären Proliferation, des Zellzykluses und der Oxidation beteiligt sind. Die Analyse der runterregulierten Gene zeigte drei wichtige molekulare funktionelle Netzwerke in der Regulation der zellulären Funktion and der Erhaltung des Karzinoms, des Zellzykluses mit der DNA-Reparatur und der posttranskriptionellen Modifizierung. Zur Bestätigung der Mikroarraydaten wurde die Expression der 8 ausgewählten differentiell exprimierten Kandidatengene, welche an der Regulation des Zellzykluses, der DNA-Schädigung und der Transkription beteiligt sind, durch qRT-PCR analysiert.

Die Ergebnisse der vorliegenden Arbeit deuteten darauf hin, dass beide Strahlenqualitäten mit biologischen Äquivalentdosen signifikante unterschiedliche Genexpressionen induzieren und dadurch die unterschiedlichen Wirkungen auf der Regulation der Signaltransduktionswege beeinflussen konnten. Die differentiell exprimierten Gene sind an der Regulation der Zellzyklen, DNA-Reparatur und der Oxidierung beteiligt. Die Identifizierung der differentiell exprimierten Gene in der vorliegenden Arbeit kann zum Verständnis der komplizierten molekularen Reaktionen auf Bestrahlung mit Kohlenstoffionen hinzufügen und wertvolle Ressource sowohl für experimentelle als auch für klinische Anwendung der Schwerionentherapie von Lungenkarzinom zur Verfügung stehen.

8. References

Abbas T, Dutta A.: p21 in cancer: intricate networks and multiple activities. *Nat Rev Cancer*. 2009 Jun;9(6):400-14.

Akino Y, Teshima T, Kihara A, Kodera-Suzumoto Y, Inaoka M, Higashiyama S, Furusawa Y, Matsuura N.: Carbon-ion beam irradiation effectively suppresses migration and invasion of human non-small-cell lung cancer cells. *Int J Radiat Oncol Biol Phys*. 2009 Oct 1;75(2):475-81.

Alizadeh AA, Eisen MB, Davis RE, Ma C, Lossos IS, Rosenwald A, Boldrick JC, Sabet H, Tran T, Yu X, Powell JI, Yang L, Marti GE, Moore T, Hudson J Jr, Lu L, Lewis DB, Tibshirani R, Sherlock G, Chan WC, Greiner TC, Weisenburger DD, Armitage JO, Warnke R, Levy R, Wilson W, Grever MR, Byrd JC, Botstein D, Brown PO, Staudt LM.: Distinct types of diffuse large B-cell lymphoma identified by gene expression profiling. *Nature*. 2000 Feb 3;403(6769):503-11.

Al-Shahrour F, Minguez P, Tarraga J, Medina I, Alloza E, Montaner D, Dopazo J.: FatiGO + : a functional profiling tool for genomic data. Integration of functional annotation, regulatory motifs and interaction data with microarray experiments. *Nucleic Acids Res*. 2007 35:W91-6.

Banin S, Moyal L, Shieh S, Taya Y, Anderson CW, Chessa L, Smorodinsky NI, Prives C, Reiss Y, Shiloh Y, Ziv Y.: Enhanced phosphorylation of p53 by ATM in response to DNA damage. *Science*. 1998 Sep 11;281(5383):1674-7.

Barrett JC, Ts'o PO.: Evidence for the progressive nature of neoplastic transformation in vitro. *Proc Natl Acad Sci U S A*. 1978 Aug;75(8):3761-5.

Bassler N, Jäkel O, Søndergaard CS, Petersen JB.: Dose- and LET-painting with particle therapy. *Acta Oncol*. 2010 Oct;49(7):1170-6.

Becker D, Elsässer T, Tonn T, Seifried E, Durante M, Ritter S, Fournier C.: Response of human hematopoietic stem and progenitor cells to energetic carbon ions. *Int J Radiat Biol.* 2009 Nov;85(11):1051-9.

Beer DG, Kardia SL, Huang CC, Giordano TJ, Levin AM, Misek DE, Lin L, Chen G, Gharib TG, Thomas DG, Lizyness ML, Kuick R, Hayasaka S, Taylor JM, Iannettoni MD, Orringer MB, Hanash S.: Gene-expression profiles predict survival of patients with lung adenocarcinoma. *Nat Med.* 2002 Aug;8(8):816-24. Epub 2002 Jul 15.

Berwanger B, Hartmann O, Bergmann E, Bernard S, Nielsen D, Krause M, Kartal A, Flynn D, Wiedemeyer R, Schwab M, Schäfer H, Christiansen H and Eilers M.: Loss of a FYN regulated differentiation and growth arrest pathway in advanced stage neuroblastoma. *Cancer Cell.* 2002 Nov;2(5):377-86.

Bhattacharjee A, Richards WG, Staunton J, Li C, Monti S, Vasa P, Ladd C, Beheshti J, Bueno R, Gillette M, Loda M, Weber G, Mark EJ, Lander ES, Wong W, Johnson BE, Golub TR, Sugarbaker DJ, Meyerson M.: Classification of human lung carcinomas by mRNA expression profiling reveals distinct adenocarcinoma subclasses. *Proc Natl Acad Sci U S A.* 2001 Nov 20;98(24):13790-5. Epub 2001 Nov 13.

Bhattacharya S, Mariani TJ.: Array of hope: expression profiling identifies disease biomarkers and mechanism. *Biochem Soc Trans.* 2009 Aug;37(Pt 4):855-62.

Blakely EA, Tobias CA, Yang TC, Smith KC, Lyman JT.: Inactivation of human kidney cells by high-energy monoenergetic heavy-ion beams. *Radiat Res.* 1979 Oct;80(1):122-60.

Bogart JA, Aronowitz JN.: Localized non-small cell lung cancer: adjuvant radiotherapy in the era of effective systemic therapy. *Clin Cancer Res.* 2005 Jul 1;11(13 Pt 2):5004s-5010s.

Chen MS, Woodward WA, Behbod F, Peddibhotla S, Alfaro MP, Buchholz TA, Rosen JM.: Wnt/beta-catenin mediates radiation resistance of Sca1+ progenitors in an immortalized mammary gland cell line. *J Cell Sci.* 2007 Feb 1;120(Pt 3):468-77.

Chen Y, Okunieff P.: Radiation and third-generation chemotherapy. *Hematol Oncol Clin North Am.* 2004 Feb;18(1):55-80.

Conrad S, Ritter S, Fournier C, Nixdorff K.: Differential effects of irradiation with carbon ions and x-rays on macrophage function. *J Radiat Res (Tokyo).* 2009 May;50(3):223-31. Epub 2009 Apr 28.

Coory M, Gkolia P, Yang IA, Bowman RV, Fong KM.: Systematic review of multidisciplinary teams in the management of lung cancer. *Lung Cancer.* 2008 Apr;60(1):14-21. Epub 2008 Mar 4. Review.

Cox R, Thacker J, Goodhead DT, Munson RJ.: Mutation and inactivation of mammalian cells by various ionising radiations. *Nature.* 1977 Jun 2;267(5610):425-7.

Curtis SB, Tenforde TS, Afzal SM.: Hypoxic cell sensitizers and heavy charged particle beams may play complementary roles in killing hypoxic tumor cells. *Int J Radiat Oncol Biol Phys.* 1984 Aug;10(8):1203-5.

Denko NC.: Hypoxia, HIF1 and glucose metabolism in the solid tumour. *Nat Rev Cancer.* 2008 Sep;8(9):705-13.

de Toledo SM, Azzam EI, Keng P, Laffrenier S, Little JB.: Regulation by ionizing radiation of CDC2, cyclin A, cyclin B, thymidine kinase, topoisomerase IIalpha, and RAD51 expression in normal human diploid fibroblasts is dependent on p53/p21Waf1. *Cell Growth Differ.* 1998 Nov;9(11):887-96.

Dewhirst MW, Cao Y, Moeller B.: Cycling hypoxia and free radicals regulate angiogenesis and radiotherapy response. *Nat Rev Cancer.* 2008 Jun;8(6):425-37

Dianov GL, O'Neill P, Goodhead DT.: Securing genome stability by orchestrating DNA repair: removal of radiation-induced clustered lesions in DNA. *Bioessays.* 2001 Aug;23(8):745-9.

Eckardt-Schupp F, Klaus C.: Radiation inducible DNA repair processes in eukaryotes.

Biochimie. 1999 Jan-Feb;81(1-2):161-71.

Erman M, Moretti L, Soria JC, Le Chevalier T, Van Houtte P.: Adjuvant chemotherapy and radiotherapy in non-small cell lung cancer. *Semin Radiat Oncol*. 2004 Oct;14(4):315-21.

Feinendegen L, Hahnfeldt P, Schadt EE, Stumpf M, Voit EO.: Systems biology and its potential role in radiobiology. *Radiat Environ Biophys*. 2008 Feb;47(1):5-23. Epub 2007 Dec 18.

Fokas E, Kraft G, An HX, Engenhardt-Cabillic R.: Ion beam radiobiology and cancer: time to update ourselves. *Biochim Biophys Acta*. 2009 Dec;1796(2):216-29. Epub 2009 Aug 12.

Fournier C, Wiese C, Taucher-Scholz G.: Accumulation of the cell cycle regulators TP53 and CDKN1A (p21) in human fibroblasts after exposure to low- and high-LET radiation. *Radiat Res*. 2004 Jun;161(6):675-84.

Franken NA, ten Cate R, Krawczyk PM, Stap J, Haveman J, Aten J, Barendsen GW.: Comparison of RBE values of high-LET α -particles for the induction of DNA-DSBs, chromosome aberrations and cell reproductive death. *Radiat Oncol*. 2011 Jun 8;6:64.

Funato Y, Michiue T, Terabayashi T, Yukita A, Danno H, Asashima M, Miki H.: Nucleoredoxin regulates the Wnt/planar cell polarity pathway in *Xenopus*. *Genes Cells*. 2008 Sep;13(9):965-75.

Furusawa Y, Fukutsu K, Aoki M, Itsukaichi H, Eguchi-Kasai K, Ohara H, Yatagai F, Kanai T, Ando K.: Inactivation of aerobic and hypoxic cells from three different cell lines by accelerated (3)He-, (12)C- and (20)Ne-ion beams. *Radiat Res*. 2000 Nov;154(5):485-96.

Fushimi K, Uzawa K, Ishigami T, Yamamoto N, Kawata T, Shibahara T, Ito H, Mizoe JE, Tsujii H, Tanzawa H.: Susceptible genes and molecular pathways related to heavy ion irradiation in oral squamous cell carcinoma cells. *Radiother Oncol*. 2008

Nov;89(2):237-44. Epub 2008 May 29.

Gademann G, Hartmann GH, Kraft G, Lorenz WJ, Wannemacher M.: The medical heavy ion therapy project at the Gesellschaft für Schwerionenforschung facility in Darmstadt. *Strahlenther Onkol.* 1990 Jan;166(1):34-9.

Gandini S, Botteri E, Iodice S, Boniol M, Lowenfels AB, Maisonneuve P, Boyle P.: Tobacco smoking and cancer: a meta-analysis. *Int J Cancer.* 2008 Jan 1;122(1):155-64.

Giard DJ, Aaronson SA, Todaro GJ, Arnstein P, Kersey JH, Dosik H, Parks WP.: In vitro cultivation of human tumors: establishment of cell lines derived from a series of solid tumors. *J. Natl. Cancer Inst.* 1973 Nov;51(5):1417-23.

Goodhead DT.: Initial events in the cellular effects of ionizing radiations: clustered damage in DNA. *Int J Radiat Biol* 1994, 65(1):7-17.

Goodhead DT.: Mechanisms for the biological effectiveness of high-LET radiations. *J Radiat Res (Tokyo)* 1999, 40 Suppl:1-13.

Goodhead DT, Thacker J, Cox R.: Weiss Lecture.: Effects of radiations of different qualities on cells: molecular mechanisms of damage and repair. *Int J Radiat Biol.* 1993 May;63(5):543-56.

Goto S, Watanabe M, Yatagai F.: Delayed cell cycle progression in human lymphoblastoid cells after exposure to high-LET radiation correlates with extremely localized DNA damage. *Radiat Res.* 2002 Dec;158(6):678-86.

Grutters JP, Kessels AG, Pijls-Johannesma M, De Ruyscher D, Joore MA, Lambin P.: Comparison of the effectiveness of radiotherapy with photons, protons and carbon-ions for non-small cell lung cancer: a meta-analysis. *Radiother Oncol.* 2010 Apr;95(1):32-40. Epub 2009 Sep 3.

Guida P, Vazquez ME, Otto S.: Cytotoxic effects of low- and high-LET radiation on human neuronal progenitor cells: induction of apoptosis and TP53 gene expression. *Radiat Res.* 2005 Oct;164(4 Pt 2):545-51.

Guo L, Ma Y, Ward R, Castranova V, Shi X, Qian Y.: Constructing molecular classifiers for the accurate prognosis of lung adenocarcinoma. *Clin Cancer Res.* 2006 Jun 1;12(11 Pt 1):3344-54.

Haasbeek CJ, Slotman BJ, Senan S.: Radiotherapy for lung cancer: Clinical impact of recent technical advances. *Lung Cancer.* 2009 Apr;64(1):1-8. Epub 2008 Sep 3.

Hamada N.: Recent insights into the biological action of heavy-ion radiation. *J Radiat Res (Tokyo).* 2009 Jan;50(1):1-9. Epub 2008 Oct 7.

Hecht SS, Kassie F, Hatsukami DK.: Chemoprevention of lung carcinogenesis in addicted smokers and ex-smokers. *Nat Rev Cancer.* 2009 Jul;9(7):476-88.

Heller G, Zielinski CC, Zöchbauer-Müller S.: Lung cancer: from single-gene methylation to methylome profiling. *Cancer Metastasis Rev.* 2010 Mar;29(1):95-107.

Hellman B, Brodin D, Andersson M, Dahlman-Wright K, Isacson U, Brattstrom D, Bergqvist M.: Radiation-induced DNA-damage and gene expression profiles in human lung cancer cells with different radiosensitivity. *Exp Oncol.* 2005 Jun;27(2):102-7.

Hennes S, Davey MW, Harvie RM, Davey RA.: Fractionated irradiation of H69 small-cell lung cancer cells causes stable radiation and drug resistance with increased MRP1, MRP2, and topoisomerase IIalpha expression. *Int J Radiat Oncol Biol Phys.* 2002 Nov 1;54(3):895-902.

Hertzberg RP, Pope AJ.: High-throughput screening: new technology for the 21st century. *Curr Opin Chem Biol.* 2000 Aug;4(4):445-51.

Higo M, Uzawa K, Kawata T, Kato Y, Kouzu Y, Yamamoto N, Shibahara T, Mizoe JE, Ito H, Tsujii H, Tanzawa H.: Enhancement of SPHK1 in vitro by carbon ion irradiation in oral squamous cell carcinoma. *Int J Radiat Oncol Biol Phys.* 2006 Jul 1;65(3):867-75.

Hirao Y.: Heavy ion synchrotron for medical use-HIMAC project at NIRS-JAPAN. *Nucl Phys.* 1992 Mar;538:541-50

Imadome K, Iwakawa M, Nojiri K, Tamaki T, Sakai M, Nakawatari M, Moritake T, Yanagisawa M, Nakamura E, Tsujii H, Imai T.: Up-regulation of stress-response genes with cell cycle arrest induced by carbon ion irradiation in multiple murine tumors models. *Cancer Biol Ther.* 2008 Feb;7(2):208-17. Epub 2007 Nov 3.

Ishikawa H, Tsuji H, Tsujii H.: Clinical experience of carbon ion radiotherapy for malignant tumors, *Gan To Kagaku Ryoho.* 2006 Apr;33(4):444-9.

Jakob B, Scholz M, Taucher-Scholz G.: Characterization of CDKN1A (p21) binding to sites of heavy-ion-induced damage: colocalization with proteins involved in DNA repair. *Int J Radiat Biol* 2002 78, 75-88.

Jakob B, Scholz M, Taucher-Scholz G. Biological imaging of heavy charged-particle tracks. *Radiat Res.* 2003 May;159(5):676-84.

Jassem J.: The role of radiotherapy in lung cancer: where is the evidence? *Radiother Oncol.* 2007 May;83(2):203-13. Epub 2007 May 4

Jeggo PA, Löbrich M.: Contribution of DNA repair and cell cycle checkpoint arrest to the maintenance of genomic stability. *DNA Repair (Amst).* 2006 Sep 8;5(9-10):1192-8.

Jemal A, Bray F, Center MM, Ferlay J, Ward E, Forman D.: Global cancer statistics. *CA Cancer J Clin.* 2011 Mar-Apr;61(2):69-90.

Jinno-Oue A, Shimizu N, Hamada N, Wada S, Tanaka A, Shinagawa M, Ohtsuki T, Mori T, Saha MN, Hoque AS, Islam S, Kogure K, Funayama T, Kobayashi Y, Hoshino H.: Irradiation with carbon ion beams induces apoptosis, autophagy, and cellular senescence in a human glioma-derived cell line. *Int J Radiat Oncol Biol Phys*. 2010 Jan 1;76(1):229-41.

Kadono K, Homma T, Kamahara K, Nakayama M, Satoh H, Sekizawa K, Miyamoto T.: Effect of heavy-ion radiotherapy on pulmonary function in stage I non-small cell lung cancer patients. *Chest*. 2002 Dec;122(6):1925-32.

Kanehisa M.: The KEGG database. *Novartis Found Symp*. 2002;247:91-101; discussion 101-3, 119-28, 244-52.

Karger CP, Jäkel O.: Current status and new developments in ion therapy. *Strahlenther Onkol*. 2007 Jun;183(6):295-300.

Kikuchi T, Daigo Y, Katagiri T, Tsunoda T, Okada K, Kakiuchi S, Zembutsu H, Furukawa Y, Kawamura M, Kobayashi K, Imai K, Nakamura Y.: Expression profiles of non-small cell lung cancers on cDNA microarrays: identification of genes for prediction of lymph-node metastasis and sensitivity to anti-cancer drugs. *Oncogene*. 2003 Apr 10;22(14):2192-205.

Koike M, Yutoku Y, Koike A.: Accumulation of p21 proteins at DNA damage sites independent of p53 and core NHEJ factors following irradiation. *Biochem Biophys Res Commun*. 2011 Aug 19;412(1):39-43. Epub 2011 Jul 20.

Kraft G.: Radiotherapy with heavy ions: radiobiology, clinical indications and experience at GSI, Darmstadt. *Tumori*. 1998 Mar-Apr;84(2):200-4.

Kraft G, Kramer M, Scholz M.: LET, track structure and models. *Radiat Environ Biophys*. 1992, 31(3):161-180.

Kurpinski K, Jang DJ, Bhattacharya S, Rydberg B, Chu J, So J, Wyrobek A, Li S, Wang D.: Differential effects of x-rays and high-energy ⁵⁶Fe ions on human

mesenchymal stem cells. *Int J Radiat Oncol Biol Phys*. 2009 Mar 1;73(3):869-77.

Li H, Sun Y, Zhan M.: Exploring pathways from gene co-expression to network dynamics. *Methods Mol Biol*. 2009;541:249-67.

Liang Y.: An expression meta-analysis of predicted microRNA targets identifies a diagnostic signature for lung cancer. *BMC Med Genomics*. 2008 Dec 16;1:61.

Liotta L, Petricoin E.: Molecular profiling of human cancer. *Nat Rev Genet*. 2000 Oct;1(1):48-56.

Livak KJ, Schmittgen TD.: Analysis of relative gene expression data using real-time quantitative PCR and the $2^{-(\Delta\Delta C(T))}$ Method. *Methods*. 2001 Dec;25(4):402-8.

Lomax AJ, Boehringer T, Coray A, Egger E, Goitein G, Grossmann M, Juelke P, Lin S, Pedroni E, Rohrer B, Roser W, Rossi B, Siegenthaler B, Stadelmann O, Stauble H, Vetter C, Wissler L.: Intensity modulated proton therapy: a clinical example. *Med Phys*. 2001 Mar;28(3):317-24.

Lu Y, Lemon W, Liu PY, Yi Y, Morrison C, Yang P, Sun Z, Szoke J, Gerald WL, Watson M, Govindan R, You M.: A gene expression signature predicts survival of patients with stage I non-small cell lung cancer. *PLoS Med*. 2006 Dec;3(12):e467.

Malumbres M, Barbacid M.: Cell cycle, CDKs and cancer: a changing paradigm. *Nat Rev Cancer*. 2009 Mar;9(3):153-66.

Minohara S, Fukuda S, Kanematsu N, Takei Y, Furukawa T, Inaniwa T, Matsufuji N, Mori S, Noda K.: Recent innovations in carbon-ion radiotherapy. *J Radiat Res (Tokyo)*. 2010;51(4):385-92. Review.

Miyamoto T, Yamamoto N, Nishimura H, Koto M, Tsujii H, Mizoe JE, Kamada T, Kato H, Yamada S, Morita S, Yoshikawa K, Kandatsu S, Fujisawa T.: Carbon ion radiotherapy for stage I non-small cell lung cancer. *Radiother Oncol*. 2003

Feb;66(2):127-40.

Murnane JP.: Cell cycle regulation in response to DNA damage in mammalian cells: a historical perspective. *Cancer Metastasis Rev.* 1995 Mar;14(1):17-29.

Nagata M, Fujita H, Ida H, Hoshina H, Inoue T, Seki Y, Ohnishi M, Ohyama T, Shingaki S, Kaji M, Saku T, Takagi R.: Identification of potential biomarkers of lymph node metastasis in oral squamous cell carcinoma by cDNA microarray analysis. *Int J Cancer.* 2003 Sep 20;106(5):683-9.

Nakano H, Shinohara K.: X-ray-induced cell death: apoptosis and necrosis. *Radiat Res.* 1994 Oct;140(1):1-9.

Nakano T, Suzuki Y, Ohno T, Kato S, Suzuki M, Morita S, Sato S, Oka K, Tsujii H.: Carbon beam therapy overcomes the radiation resistance of uterine cervical cancer originating from hypoxia. *Clin Cancer Res.* 2006 Apr 1;12(7 Pt 1):2185-90.

Nasonova E, Füssel K, Berger S, Gudowska-Nowak E, Ritter S.: Cell cycle arrest and aberration yield in normal human fibroblasts. I. Effects of X-rays and 195 MeV u(-1) C ions. *Int J Radiat Biol.* 2004 Sep;80(9):621-34.

Nihei K, Ogino T, Ishikura S, Nishimura H.: High-dose proton beam therapy for Stage I non-small-cell lung cancer. *Int J Radiat Oncol Biol Phys.* 2006 May 1;65(1):107-11. Epub 2006 Feb 3.

Nojiri K, Iwakawa M, Ichikawa Y, Imadome K, Sakai M, Nakawatari M, Ishikawa K, Ishikawa A, Togo S, Tsujii H, Shimada H, Imai T.: The proangiogenic factor ephrin-A1 is up-regulated in radioresistant murine tumor by irradiation. *Exp Biol Med (Maywood).* 2009 Jan;234(1):112-22. Epub 2008 Nov 7.

Okada T, Kamada T, Tsuji H, Mizoe JE, Baba M, Kato S, Yamada S, Sugahara S, Yasuda S, Yamamoto N, Imai R, Hasegawa A, Imada H, Kiyohara H, Jingu K, Shinoto M, Tsujii H.: Carbon ion radiotherapy: clinical experiences at National Institute of Radiological Science (NIRS). *J Radiat Res (Tokyo).* 2010;51(4):355-64.

Epub 2010 May 28.

Ohnishi K, Ohnishi T.: The biological effects of space radiation during long stays in space. *Biol Sci Space*. 2004 Dec;18(4):201-5.

Ostroff RM, Bigbee WL, Franklin W, Gold L, Mehan M, Miller YE, Pass HI, Rom WN, Siegfried JM, Stewart A, Walker JJ, Weissfeld JL, Williams S, Zichi D, Brody EN.: Unlocking biomarker discovery: large scale application of aptamer proteomic technology for early detection of lung cancer. *PLoS One*. 2010 Dec 7;5(12):e15003.

Pijls-Johannesma M., Grutters J, Lambin P, Ruyscher D.: Particle therapy in lung cancer: Where do we stand? *Cancer Treat Rev*. 2008 May;34(3):259-67. Epub 2008 Jan 15.

Potti A, Mukherjee S, Petersen R, Dressman HK, Bild A, Koontz J, Kratzke R, Watson MA, Kelley M, Ginsburg GS, West M, Harpole DH Jr, Nevins JR.: A genomic strategy to refine prognosis in early-stage non-small-cell lung cancer. *N Engl J Med*. 2006 Aug 10;355(6):570-80.

Poulsen TT, Pedersen N, Perin MS, Hansen CK, Poulsen HS.: Specific sensitivity of small cell lung cancer cell lines to the snake venom toxin taipoxin. *Lung Cancer*. 2005 Dec;50(3):329-37. Epub 2005 Aug 22.

PTCOG: <http://ptcog.web.psi.ch/>

Qanungo S, Starke DW, Pai HV, Mieyal JJ, Nieminen AL.: Glutathione supplementation potentiates hypoxic apoptosis by S-glutathionylation of p65-NFkappaB. *J Biol Chem*. 2007 Jun 22;282(25):18427-36. Epub 2007 Apr 27.

Ramaswamy S, Ross KN, Lander ES, Golub TR.: A molecular signature of metastasis in primary solid tumors. *Nat Genet*. 2003 Jan;33(1):49-54. Epub 2002 Dec 9.

Rengan R, Maity AM, Stevenson JP, Hahn SM.: New strategies in non-small cell lung cancer: improving outcomes in chemoradiotherapy for locally advanced disease. *Clin*

Cancer Res. 2011 Jul 1;17(13):4192-9. Epub 2011 May 16.

Rosell R, Cecere F, Santarpia M, Reguart N, Taron M.: Predicting the outcome of chemotherapy for lung cancer. *Curr Opin Pharmacol.* 2006 Aug;6(4):323-31. Epub 2006 Jun 12.

Roy D, Guida P, Zhou G, Echiburu-Chau C, Calaf GM.: Gene expression profiling of breast cells induced by X-rays and heavy ions. *Int J Mol Med.* 2008 May;21(5):627-36.

Sambrook J, Fritsche EF, Maniatis T.: *Molecular Cloning - A Laboratory Manual*, 1989, 2nd Ed.

Scholz M, Kraft-Weyrather W, Ritter S, Kraft G.: Cell cycle delays induced by heavy ion irradiation of synchronous mammalian cells. *Int J Radiat Biol.* 1994 Jul;66(1):59-75.

Schulz-Ertner D, Tsujii H.: Particle radiation therapy using proton and heavier ion beams. *J Clin Oncol.* 2007 Mar 10;25(8):953-64.

Scott WJ, Howington J, Feigenberg S, Movsas B, Pisters K.: Treatment of non-small cell lung cancer stage I and stage II: ACCP evidence-based clinical practice guidelines. *Chest.* 2007 Sep;132(3 Suppl):234S-242S.

Shioyama Y, Tokuyue K, Okumura T, Kagei K, Sugahara S, Ohara K, Akine Y, Ishikawa S, Satoh H, Sekizawa K.: Clinical evaluation of proton radiotherapy for non-small-cell lung cancer. *Int J Radiat Oncol Biol Phys.* 2003 May 1;56(1):7-13.

Singhal S, Miller D, Ramalingam S, Sun SY.: Gene expression profiling of non-small cell lung cancer. *Lung Cancer.* 2008 Jun;60(3):313-24. Epub 2008 Apr 25.

Singleton BK, Griffin CS, Thacker J.: Clustered DNA damage leads to complex genetic changes in irradiated human cells. *Cancer Res.* 2002 Nov 1;62(21):6263-9.

Skarsgard LD: Radiobiology with heavy charged particles: a historical review. *Phys Med* 1998, 14 Suppl 1:1-19.

Sørensen BS, Overgaard J, Bassler N.: In vitro RBE-LET dependence for multiple particle types. *Acta Oncol.* 2011 Aug;50(6):757-62.

Starmans MH, Krishnapuram B, Steck H, Horlings H, Nuyten DS, van de Vijver MJ, Seigneuric R, Buffa FM, Harris AL, Wouters BG, Lambin P.: Robust prognostic value of a knowledge-based proliferation signature across large pati microarray studies spanning different cancer types. *Br J Cancer.* 2008 Dec 2;99(11):1884-90. Epub 2008 Nov 4.

Stone RS.: Neutron therapy and specific ionization. *Am J Roentgenol Radium Ther.* 1948 Jun;59(6):771-85

Streit S, Michalski CW, Erkan M, Friess H, Kleeff J.: Confirmation of DNA microarray-derived differentially expressed genes in pancreatic cancer using quantitative RT-PCR. *Pancreatology.* 2009;9(5):577-82.

Suzuki M, Kase Y, Yamaguchi H, Kanai T, Ando K.: Relative biological effectiveness for cell-killing effect on various human cell lines irradiated with heavy-ion medical accelerator in Chiba (HIMAC) carbon-ion beams. *Int J Radiat Oncol Biol Phys.* 2000 Aug 1;48(1):241-50.

Tamaki T, Iwakawa M, Ohno T, Imadome K, Nakawatari M, Sakai M, Tsujii H, Nakano T, Imai T.: Application of carbon-ion beams or gamma-rays on primary tumors does not change the expression profiles of metastatic tumors in an in vivo murine model. *Int J Radiat Oncol Biol Phys.* 2009 May 1;74(1):210-8.

Terasawa T, Balk EM, Chung M, Garlitski AC, Alsheikh-Ali AA, Lau J, Ip S.: Systematic review: comparative effectiveness of radiofrequency catheter ablation for atrial fibrillation. *Ann Intern Med.* 2009 Aug 4;151(3):191-202. Epub 2009 Jul 6..

Tobias CA, Anger HO, Lawrence JH.: Radiological use of high energy deuterons and alpha particles. *Am J Roentgenol Radium Ther Nucl Med.* 1952 Jan;67(1):1-27.

Trevino V, Falciani F, Barrera-Saldaña HA.: DNA microarrays: a powerful genomic tool for biomedical and clinical research. *Mol Med*. 2007 Sep-Oct;13(9-10):527-41.

van't Veer LJ, Paik S, Hayes DF.: Gene expression profiling of breast cancer: a new tumor marker. *J Clin Oncol*. 2005 Mar 10;23(8):1631-5.

Wang J, Qiu X, Kulkarni A, Hauer-Jensen M.: Calcitonin gene-related peptide and substance P regulate the intestinal radiation response. *Clin Cancer Res*. 2006 Jul 1;12(13):4112-8.

Weyrather WK, Kraft G.: RBE of carbon ions: experimental data and the strategy of RBE calculation for treatment planning. *Radiother Oncol*. 2004 Dec;73 Suppl 2:S161-9.

Wilson RR.: Radiological use of fast protons. *Radiology*. 1946 Nov;47(5):487-91.

Yashiro T, Koyama-Saegusa K, Imai T, Fujisawa T, Miyamoto T.: Inhibition of potential lethal damage repair and related gene expression after carbon-ion beam irradiation to human lung cancer grown in nude mice. *J Radiat Res (Tokyo)*. 2007 Sep;48(5):377-83. Epub 2007 Aug 8

Zhang YW, Jones TL, Martin SE, Caplen NJ, Pommier Y.: Implication of checkpoint kinase-dependent up-regulation of ribonucleotide reductase R2 in DNA damage response. *J Biol Chem*. 2009 Jul 3;284(27):18085-95. Epub 2009 May 5.

9. Appendix

9.1. List of Figures

Fig.1. Schematic diagram of Bragg Peak.....	8
Fig.2. Relationship of linear energy transfer (LET, 100 KeV/ μ m) and Relative Biologic Effectiveness (RBE) for carbon ions.....	8
Fig.3. Radiation induced a serials of biological responses progressed in different levels.....	13
Fig.4. Schematic representation of a gene expression microarray assay.....	17
Fig.5. Overview of the utility of gene expression microarray technology in lung cancer diseases biomarker and therapeutic target discovery.....	18
Fig.6. BIBA (Biologische Bestrahlungs-Anlage) facility in GSI, Darmstadt.....	28
Fig.7. Survival curves of A549 cells after irradiation with carbon ion and X-ray..	34
Fig.8. Quality control of RNA by agarose gel electrophoresis.....	36
Fig.9. Scatter plots of median signal intensities of microarray data obtained from two channels.....	37
Fig.10. Interrelated networks of genes whose expression was modified after carbon ion irradiation.....	43
Fig.11A. Network 1 (cellular proliferation) of up-regulated genes between carbon ion and X-ray irradiation.....	49
Fig.11B. Network 2 (cell cycle regulation) of up-regulated genes between carbon and X-ray irradiation.....	50
Fig.11C Network 3 (oxidation reduction) of up-regulated genes between carbon ion and X-ray irradiation.....	51
Fig.12A. Network 1 (cellular function and maintenance of cancer) of down-regulated genes between carbon ion and X-ray irradiation.....	52
Fig.12B. Network 2 (cell cycle regulation) of down-regulated genes between carbon ion and X-ray irradiation.....	53
Fig.12C. Network 3 (post translation modification) of down-regulated genes between carbon ion and X-ray irradiation.....	54
Fig.13. Determination and comparison of the qRT-PCR efficiency for GAPDH and candidate (CCND2).....	55

Fig.14. Validation of selected genes in A549 cells 4 h after heavy ion beam and X-ray irradiation using qRT-PCR..... 58

9.2. List of Tables

Table.1. Primer sequences and PCR conditions.....	22
Table.2. Merged genetic networks identified in A549 cells irradiated with carbon ion.....	40
Table.3. canonical pathways in carbon ion-irradiated genes.....	42
Table.4. Genetic networks of up-regulated genes between carbon ion and X-ray	46
Table.5. Genetic networks of down-regulated genes between carbon ion and X-ray.....	47
Table.6. Canonical pathways of the differentially expressed genes.....	48
Table 7. Functions of selected genes selected for the validation of microarray results.....	57

9.3. Genes significantly up-regulated by carbon ion beam irradiation

Symbol	Entrez Gene ID	Gene Name
ABCC5	10057	ATP-binding cassette, sub-family C (CFTR/MRP), member 5
APBA2	321	amyloid beta (A4) precursor protein-binding, family A, member 2
B3GAT3	26229	beta-1,3-glucuronyltransferase (glucuronosyltransferase I) 3
C11ORF51	25906	chromosome 11 open reading frame 51
CAMK1D	57118	calcium/calmodulin-dependent protein kinase ID
CCND2	894	cyclin D2
CD70	970	CD70 molecule
CDC14B	8555	CDC14 cell division cycle 14 homolog B
CDC42EP1	11135	CDC42 effector protein (Rho GTPase binding) 1
CTBS	1486	chitobiase, di-N-acetyl
DDB2	1643	damage-specific DNA binding protein 2
DHPS	1725	deoxyhypusine synthase
E2F5	1875	E2F transcription factor 5, p130-binding
FAM179B	23116	family with sequence similarity 179, member B
GAP43	2596	growth associated protein 43
HBEGF	1839	heparin-binding EGF-like growth factor
HIC2	23119	hypermethylated in cancer 2
HNRNPR	10236	heterogeneous nuclear ribonucleoprotein R
HPS1	3257	Hermansky-Pudlak syndrome 1
PLEKHG3	26030	pleckstrin homology domain containing, family G (with RhoGef domain) member 3
POLS	11044	PAP-associated domain-containing protein 7
PPHLN1	51535	periphilin 1
RNF219	79596	ring finger protein 219
SFXN3	81855	sideroflexin 3
THRB	7068	thyroid hormone receptor, beta

TIMP	7076	TIMP metalloproteinase inhibitor 1
TIMP3	7078	TIMP metalloproteinase inhibitor 3
TRIM32	22954	tripartite motif containing 32
APBA2	321	amyloid beta (A4) precursor protein-binding, family A, member 2

9.4. Genes significantly down-regulated by carbon ion beam irradiation

Symbol	Entrez Gene ID	Gene Name
BTBD10	84280	BTB (POZ) domain containing 10
C9ORF75	286262	chromosome 9 open reading frame 75
CDC42BPA	8476	CDC42 binding protein kinase alpha (DMPK-like)
DCTPP1	79077	dCTP pyrophosphatase 1
FGFR1OP2	26127	FGFR1 oncogene partner 2
NPHP4	261734	nephronophthisis 4
OAZ2	4947	ornithine decarboxylase antizyme 2
PHKA2	5256	phosphorylase kinase, alpha 2 (liver)
PPM1D	8493	protein phosphatase, Mg ²⁺ /Mn ²⁺ dependent, 1D
PPME1	51400	protein phosphatase methylesterase 1
OAZ2	4947	ornithine decarboxylase antizyme 2
PCTK3	5129	PTCTAIRE-motif protein kinase 3
RARG	5916	retinoic acid receptor, gamma
RIPK4	54101	receptor-interacting serine-threonine kinase 4
RPL21	6144	ribosomal protein L21
SH2B1	25970	SH2B adaptor protein 1
SNRPG	6637	small nuclear ribonucleoprotein polypeptide G
SYDE1	85360	synapse defective 1, Rho GTPase, homolog 1 (C. elegans)
TAX1BP1	8887	Tax1 (human T-cell leukemia virus type I) binding protein 1
TSPAN17	26262	tetraspanin 17

9.5. List of genes up-regulated by carbon ion beam irradiation compared to X-ray

Symbol	Entrez Gene ID	Gene Name
ABCF2	10061	ATP-binding cassette, sub-family F, member 2
ACLY	47	ATP citrate lyase
ACTA2	59	Actin, alpha 2, smooth muscle, aorta
ACTG2	72	Actin, gamma 2, smooth muscle, enteric
ADAM11	4185	ADAM metalloproteinase domain 11
ADAM15	8751	ADAM metalloproteinase domain 15
AFAP1	60312	Actin filament associated protein 1
AGAP2	116986	ArfGAP with GTPase domain
AMOTL2	51421	Angiomotin like 2
ANKRA2	57763	Ankyrin repeat, family A (RFXANK-like), 2
ANXA5	308	Annexin A5
ASB1	51665	Ankyrin repeat and SOCS box-containing 1
ASXL1	171023	Additional sex combs like 1
ATP2B3	492	ATPase, Ca ⁺⁺ transporting, plasma membrane 3
ATP5G2	517	ATP synthase, mitochondrial Fo complex, subunit C2
AURKA	6790	Aurora kinase A
AURKB	9212	Aurora kinase B
AUTS2	26053	Autism susceptibility candidate 2
BGN	633	Biglycan
BIRC5	332	Baculoviral IAP repeat-containing 5 (survivin)
BMS1	9790	BMS1 homolog, ribosome assembly protein
CACYBP	27101	Calcyclin binding protein
CAMSAP1	157922	Calmodulin regulated spectrin-associated protein 1
CAMSAP1L1	23271	Calmodulin regulated spectrin-associated protein 1-like 1
CCDC43	124808	Coiled-coil domain containing 43
CCNB1	891	Cyclin B1
CCND2	894	cyclin D2
CCT4	10575	Chaperonin containing TCP1, subunit 4 (delta)

CDC14B	8555	CDC14 cell division cycle 14 homolog B
CDC2	983	Cell division cycle 2, G1 to S and G2 to M
CDC6	990	Cell division cycle 6 homolog (<i>S. cerevisiae</i>)
CDCA5	113130	Cell division cycle associated 5
CDKN1A	1026	Cyclin-dependent kinase inhibitor 1A (p21)
CENPF	1063	Centromere protein F, 350/400ka (mitosin)
CHAF1B	8208	Chromatin assembly factor 1, subunit B (p60)
COTL1	23406	Coactosin-like 1 (<i>Dictyostelium</i>)
COX10	1352	Cytochrome c oxidase assembly protein
CPSF6	11052	Cleavage and polyadenylation specific factor 6, 68kDa
CTPS	1503	CTP synthase
CUL4A	8451	Cullin 4A
CYB5R4	51167	Cytochrome b5 reductase 4
CYFIP2	26999	Cytoplasmic FMR1 interacting protein 2
DCUN1D5	84259	DCN1, defective in cullin neddylation 1, domain containing 5 (<i>S. cerevisiae</i>)
DDEF1	50807	Development and differentiation enhancing factor 1
DDX41	51428	DEAD (Asp-Glu-Ala-Asp) box polypeptide 41
DDX46	9879	DEAD (Asp-Glu-Ala-Asp) box polypeptide 46
DHX8	1659	DEAH (Asp-Glu-Ala-His) box polypeptide 8
DKC1	1736	Dyskeratosis congenita 1, dyskerin
DTYMK	1841	Deoxythymidylate kinase (thymidylate kinase)
E2F5	1875	E2F transcription factor 5
EED	8726	Embryonic ectoderm development
EIF2C2	27161	Eukaryotic translation initiation factor 2C, 2
ELAV	1994	(embryonic lethal, abnormal vision, <i>Drosophila</i>)-like 1
EMP2	2013	Epithelial membrane protein 2
EPC1	80314	Enhancer of polycomb homolog 1 (<i>Drosophila</i>)
EPHB6	2051	EPH receptor B6
EYA2	2139	Eyes absent homolog 2 (<i>Drosophila</i>)

EZH2	2146	Enhancer of zeste homolog 2 (<i>Drosophila</i>)
FAM43A	131583	Family with sequence similarity 43, member A
FAM44B	91272	Family with sequence similarity 44, member B
FAM83D	81610	Family with sequence similarity 83, member D
FAM84A	151354	Family with sequence similarity 84, member A
FARP1	10160	FERM, RhoGEF and pleckstrin domain protein 1
FARSA	2193	Phenylalanyl-tRNA synthetase, alpha subunit
FAS	355	Fas (TNF receptor superfamily, member 6)
FEN1	2237	Flap structure-specific endonuclease 1
FEZ2	9637	Fasciculation and elongation protein zeta 2 (zygin II)
FGFR1	2260	Fibroblast growth factor receptor 1 (fms-related tyrosine kinase 2, Pfeiffer syndrome)
FJX1	24147	Four jointed box 1
FLNA	2316	Filamin A, alpha
GALNT13	114805	UDP-N-acetyl-alpha-D-galactosamine:polypeptide N-acetylgalactosaminyltransferase 13
GDAP1	54332	Ganglioside-induced differentiation-associated protein 1
GEM	2669	GTP binding protein overexpressed in skeletal muscle
GLDC	2731	Glycine dehydrogenase (decarboxylating)
GPR116	221395	G protein-coupled receptor 116
GTPBP4	23560	GTP binding protein 4
H2AFX	3014	H2A histone family, member X
HEATR2	54919	HEAT repeat containing 2
HERC4	26091	Hect domain and RLD 4
HIPK2	28996	Homeodomain interacting protein kinase 2
HMGB3	3149	High-mobility group box 3
HNRNPU	3192	Heterogeneous nuclear ribonucleoprotein U
HSPB8	26353	Heat shock 22kDa protein 8
HSPH1	10808	Heat shock 105kDa/110kDa protein 1
IFT88	8100	Intraflagellar transport 88 homolog (<i>Chlamydomonas</i>)
ILF3	3609	Interleukin enhancer binding factor 3, 90kDa
KCNA1	3736	Potassium voltage-gated channel, shaker-related

		subfamily, member 1
KDM2A	22992	Lysine (K)-specific demethylase 2A
KLK10	5655	Kallikrein-related peptidase 10
KNTC1	9735	Kinetochore associated 1
KRT7	3855	Keratin 7
LMNB2	84823	Lamin B2
LSM14A	26065	SCD6 homolog A
MAD2L1	4085	MAD2 mitotic arrest deficient-like 1
MAMLD1	10046	Mastermind-like domain containing 1
MAPRE1	22919	Microtubule-associated protein, RP/EB family, member 1
MBNL3	55796	Muscleblind-like 3 (Drosophila)
MPO	4353	Myeloperoxidase
MYC	4609	V-myc myelocytomatosis viral oncogene homolog (avian)
NCAPH	23397	Non-SMC condensin I complex, subunit H
NCOA3	8202	Nuclear receptor coactivator 3
NEK6	10783	NIMA (never in mitosis gene a)-related kinase 6
NET1	10276	Neuroepithelial cell transforming gene 1
NUDT13	2596	Nudix -type motif 13
NUP85	79902	Nucleoporin 85kDa
NUP93	9688	Nucleoporin 93kDa
NXN	64359	Nucleoredoxin
ODC1	4953	Ornithine decarboxylase 1
OLFML2A	169611	Olfactomedin-like 2A
PAH	5053	Phenylalanine hydroxylase
PDXP	57026	Pyridoxal (pyridoxine, vitamin B6) phosphatase
PLEKHG3	26030	Pleckstrin homology domain containing, family G, member 3
PLK1	5347	Polo-like kinase 1
PNN	5411	Pinin, desmosome associated protein
POLA2	23649	Polymerase (DNA directed), alpha 2 (70kD subunit)
PPM1D	8493	Protein phosphatase 1D magnesium-dependent, delta

		isoform
PPP1R14A	94274	Protein phosphatase 1, regulatory (inhibitor) subunit 14A
PRKAG2	51422	Protein kinase, AMP-activated, gamma 2 non-catalytic subunit
PRKAR1A	5573	Protein kinase alpha (tissue specific extinguisher 1)
PRSS23	11098	Protease, serine, 23
PSMD12	5718	Proteasome, 26S subunit, non-ATPase, 12
PSPC1	55269	Paraspeckle component 1
PTBP1	5725	Polypyrimidine tract binding protein 1
PTPRJ	5795	Protein tyrosine phosphatase, receptor type, J
PTRF	284119	Polymerase I and transcript release factor
RAD18	56852	RAD18 homolog (<i>S. cerevisiae</i>)
RAMP1	10267	Receptor (G protein-coupled) activity modifying protein 1
RARRES3	5920	Retinoic acid receptor responder 3
RBM14	10432	RNA binding motif protein 14
RBM3	5935	RNA binding motif (RNP1, RRM) protein 3
REV1	51455	REV1 homolog
RFC4	5984	Replication factor C (activator 1) 4, 37kDa
RPIA	22934	Ribose 5-phosphate isomerase A
RRM2	6241	Ribonucleotide reductase M2 polypeptide
RSU1	6251	Ras suppressor protein 1
SAE2	10054	SUMO1 activating enzyme subunit 2
SDCCAG3	10807	Serologically defined colon cancer antigen 3
SESN3	143686	Sestrin 3
SF1	7536	Splicing factor 1
SF3B5	83443	Splicing factor 3b, subunit 5, 10kDa
SFRP1	6422	Secreted frizzled-related protein 1
SFRS2B	10929	Splicing factor, arginine/serine-rich 2B
SLC26A2	1836	Solute carrier family 26 (sulfate transporter), member 2

SLC31A2	1318	Solute carrier family 31 (copper transporters), member 2
SLC6A16	28968	Solute carrier family 6, member 16
SLC7A5	8140	Solute carrier family 7 (cationic amino acid transporter), member 5
SMAD4	4089	SMAD family member 4
SRR	63826	Serine racemase
STX2	2054	Syntaxin 2
SYDE1	85360	Synapse defective 1, Rho GTPase, homolog 1 (C. elegans)
SYNCRIP	10492	Synaptotagmin binding, cytoplasmic RNA interacting protein
TARDBP	23435	TAR DNA binding protein
TAX1BP3	30851	Tax1 (human T-cell leukemia virus type I) binding protein 3
TMEPAI	56937	Transmembrane, prostate androgen induced RNA
TNS3	64759	Tensin 3
TOM1	10043	Target of myb1 (chicken)
TOP2A	7153	Topoisomerase (DNA) II alpha 170kDa
TRIM15	89870	Tripartite motif-containing 15
TSFM	10102	Ts translation elongation factor, mitochondrial
TSPAN15	23555	Tetraspanin 15
TUBGCP3	10426	Tubulin, gamma complex associated protein 3
TXNDC1	81542	Thioredoxin domain containing 1
UBE2G1	7326	ubiquitin-conjugating enzyme E2G 1
WDR57	9410	WD repeat domain 57 (U5 snRNP specific)
WDR77	79084	WD repeat domain 77
YLPM1	56252	YLP motif containing 1
YWHAH	7533	Tyrosine 3-monooxygenase/tryptophan 5-monooxygenase activation protein, eta polypeptide
YWHAZ	7534	Tyrosine 3-monooxygenase/tryptophan 5-monooxygenase activation protein, zeta polypeptide
ZFAND5	7763	Zinc finger, AN1-type domain 5

ZNF30	90075	Zinc finger protein 30
ZNF532	55205	Zinc finger protein 532
ZWILCH	55055	Zwilch, kinetochore associated, homolog (Drosophila)
ZXDC	79364	ZXD family zinc finger C

9.6. List of genes down-regulated by carbon ion beam irradiation compared to X-ray

Symbol	Entrez Gene ID	Gene Name
ACOX1	51	Acyl-Coenzyme A oxidase 1, palmitoyl
ACSL6	23305	Acyl-CoA synthetase long-chain family member 6
ADH6	130	Alcohol dehydrogenase 6 (class V)
ADSSL1	122622	Adenylosuccinate synthase like 1
AGTRAP	57085	Angiotensin II receptor-associated protein
AHSA2	130872	Activator of heat shock 90kDa protein ATPase homolog 2
AKAP1	8165	A kinase (PRKA) anchor protein 1
ANG	283	Angiogenin, ribonuclease, RNase A family, 5
ANKRD38	163782	Ankyrin repeat domain 38
APOH	350	Apolipoprotein H (beta-2-glycoprotein I)
APOL1		APOL1
AQP3	360	Aquaporin 3 (Gill blood group)
ART4	420	ADP-ribosyltransferase 4 (Dombrock blood group)
ATN1	1822	Atrophin 1
AURKAIP1	54998	Aurora kinase A interacting protein 1
BAI3		Brain-specific angiogenesis inhibitor 3
BCL2A1	597	BCL2-related protein A1
CA3	761	Carbonic anhydrase III, muscle specific
CAMK2N1	55450	Calcium/calmodulin-dependent protein kinase II inhibitor 1
CCL2	6347	Chemokine (C-C motif) ligand 2
CCL4L2	388372	Chemokine (C-C motif) ligand 4-like 2
CD55	1604	CD55 molecule, decay accelerating factor for complement
CDC25B	994	Cell division cycle 25 homolog B
CDH1	999	Cadherin 1, type 1, E-cadherin (epithelial)

CDKN1B	1027	cyclin-dependent kinase inhibitor 1B (p27)
CEP68	23177	Centrosomal protein 68kDa
CNTN1	1272	Contactin 1
COL5A1	1289	Collagen, type V, alpha 1
COMM6	170622	COMM domain containing 6
COMP	1311	Cartilage oligomeric matrix protein
CP	1356	Ceruloplasmin (ferroxidase)
CXCL1	2919	Chemokine (C-X-C motif) ligand 1
CYB5A	1528	Cytochrome b5 type A (microsomal)
CYP27A1	1593	Cytochrome P450, family 27, subfamily A, polypeptide 1
DHRS3	9249	Dehydrogenase/reductase (SDR family) member 3
DIO2	1734	Deiodinase, iodothyronine, type II
DLGAP4	22839	Discs, large (Drosophila) homolog-associated protein 4
DNAJB9	4189	DnaJ (Hsp40) homolog, subfamily B, member 9
DNAJC4	3338	DnaJ (Hsp40) homolog, subfamily C, member 4
DR1	1810	Down-regulator of transcription 1, TBP-binding (negative cofactor 2)
ERLEC1	27248	Endoplasmic reticulum lectin 1
ETFB	2109	Electron-transfer-flavoprotein, beta polypeptide
FAF1	11124	Fas (TNFRSF6) associated factor 1
FAM80B	57494	Family with sequence similarity 80, member B
FETUB	26998	Fetuin B
FGFRL1	53834	Fibroblast growth factor receptor-like 1
FKBP2	2286	FK506 binding protein 2, 13kDa
FN1	2335	Fibronectin 1
FRAS1		FRAS1
FUCA1		FUCA1
FVT1	2531	Follicular lymphoma variant translocation 1
GABARAPL1	23710	GABA(A) receptor-associated protein like 1
GABPA	2551	GA binding protein transcription factor, alpha

		subunit 60kDa
GFM1	85476	G elongation factor, mitochondrial 1
GIYD2	79008	GIY-YIG domain containing 2
GK2	2712	Glycerol kinase 2
GLIPR1	11010	GLI pathogenesis-related 1 (glioma)
GLRX	2745	Glutaredoxin (thioltransferase)
GNAO1	2775	Guanine nucleotide binding protein (G protein), alpha activating activity polypeptide O
GOLGA2	2801	Golgi autoantigen, golgin subfamily a, 2
GPX2	2877	Glutathione peroxidase 2 (gastrointestinal)
GTF2B	2959	General transcription factor IIB
HIST1H1C	3006	Histone cluster 1, H1c
HIST2H2BE	8349	Histone cluster 2, H2be
HMGN3	9324	High mobility group nucleosomal binding domain 3
HSD17B8	7923	Hydroxysteroid (17-beta) dehydrogenase 8
HYAL1	3373	Hyaluronoglucosaminidase 1
IFITM2	3459	Interferon gamma receptor 1
IFNGR1	10581	Interferon induced transmembrane protein 2 (1-8D)
IGF1R	3480	Insulin-like growth factor 1 receptor
IGFBP1	3484	Insulin-like growth factor binding protein 1
IGFBP3	3486	Insulin-like growth factor binding protein 3
IGFBP6	3489	Insulin-like growth factor binding protein 6
IL32	9235	Interleukin 32
INSL4	3641	Insulin-like 4 (placenta)
IPCEF1	26034	interaction protein for cytohesin exchange factors 1
IQGAP2	10788	IQ motif containing GTPase activating protein 2
IRF2	3660	Interferon regulatory factor 2
IRF2BP2	359948	Interferon regulatory factor 2 binding protein 2
IRF8	3394	Interferon regulatory factor 8
IRF9	10379	Interferon regulatory factor 9

ISG15	9636	ISG15 ubiquitin-like modifier
ISG20	3669	Interferon stimulated exonuclease gene 20kDa
JMJD3	23135	Jumonji domain containing 3
KANK4	163782	KN motif and ankyrin repeat domains 4
KLHDC8B	200942	kelch domain containing 8B
LGALS3BP	3959	Lectin, galactoside-binding, soluble, 3 binding protein
LRRC56	115399	Leucine rich repeat containing 56
LTB4DH	22949	Leukotriene B4 12-hydroxydehydrogenase
MALAT1	378938	Metastasis associated lung adenocarcinoma transcript 1
MAPK1	5594	Mitogen-activated protein kinase 1
MAPK4	5596	Mitogen-activated protein kinase 4
METTL7A	25840	Methyltransferase like 7A
METTL10	399818	Methyltransferase like 10
MFAP5	8076	Microfibrillar associated protein 5
MMP15	4324	Matrix metalloproteinase 15
MOBKL2C	148932	MOB1, Mps One Binder kinase activator-like 2C (yeast)
MPP7	143098	Membrane protein, palmitoylated 7 (MAGUK p55 subfamily member 7)
MSX2		MSH homeobox 2
MX1	4599	Myxovirus (influenza virus) resistance 1, interferon-inducible protein p78 (mouse)
MYL6B	140465	Myosin, light chain 6B, alkali, smooth muscle and non-muscle
NCSTN	23385	Nicastrin
NDUFB1	4707	NADH dehydrogenase (ubiquinone) 1 beta subcomplex, 1, 7kDa
NICN1	84276	Nicolin 1
NRARP	441478	NOTCH-regulated ankyrin repeat protein
NRP2	8828	Neuropilin 2
NXF1	10482	Nuclear RNA export factor 1

OAZ2	4947	Ornithine decarboxylase antizyme 2
PAPPA	5069	Pregnancy-associated plasma protein A, pappalysin 1
PDGFRL	5157	Platelet-derived growth factor receptor-like
PDK4	5166	Pyruvate dehydrogenase kinase, isozyme 4
PFDN5	5204	Prefoldin subunit 5
PLSCR1	5359	Phospholipid scramblase 1
PLXNA2	5362	Plexin A2
PNKD	25953	Paroxysmal nonkinesigenic dyskinesia
PNPLA4	8228	Patatin-like phospholipase domain containing 4
POLD4	57804	Polymerase (DNA-directed), delta 4
POLR1D	51082	Polymerase (RNA) I polypeptide D, 16kDa
PON3	5446	Paraoxonase 3
PPWD1	23398	Peptidylprolyl isomerase domain and WD repeat containing 1
PRRG4	79056	Proline rich Gla (G-carboxyglutamic acid) 4
PSME1	5720	Proteasome (prosome, macropain) activator subunit 1 (PA28 alpha)
PSME2	5721	Proteasome (prosome, macropain) activator subunit 2 (PA28 beta)
PTGS2	5743	Prostaglandin-endoperoxide synthase 2
RAB31	11031	RAB31, member RAS oncogene family
RAP1GDS1	5910	RAP1, GTP-GDP dissociation stimulator 1
RARB	5915	Retinoic acid receptor, beta
RARG	5916	Retinoic acid receptor, gamma
RARRES1	5918	Retinoic acid receptor responder (tazarotene induced) 1
RBPJ	3516	Recombination signal binding protein for immunoglobulin kappa J region
S100P	6286	S-100P PROTEIN
SAT1	6303	Spermidine/spermine N1-acetyltransferase 1
SCNN1A	6337	Sodium channel, nonvoltage-gated 1 alpha
SERINC2	347735	Serine incorporator 2

SERPINB1	1992	Serpin peptidase inhibitor, clade B (ovalbumin), member 1
SHROOM1	134549	Shroom family member 1
SIP1	8487	Survival of motor neuron protein interacting protein 1
SLC16A3	9123	Solute carrier family 16, member 3 (monocarboxylic acid transporter 4)
SLC23A2	9962	Solute carrier family 23 (nucleobase transporters), member 2
SLC25A29	123096	Solute carrier family 25, member 29
SLC29A4	222962	Solute carrier family 29 (nucleoside transporters), member 4
SLC36A4	120103	Solute carrier family 36 (proton/amino acid symporter), member 4
SLC7A2	6542	solute carrier family 7 (cationic amino acid transporter), member 2
SLC7A7	9056	Solute carrier family 7 (cationic amino acid transporter), member 7
SMPDL3A	10924	Sphingomyelin phosphodiesterase, acid-like 3A
SNHG7	84973	Small nucleolar RNA host gene (non-protein coding) 7
SOD2	6648	Superoxide dismutase 2, mitochondrial
SP100	6672	SP100 nuclear antigen
ST3GAL4	6484	ST3 beta-galactoside alpha-2,3-sialyltransferase 4
STX17	55014	syntaxin 17
SYNPO2L	79933	Synaptopodin 2-like
TBC1D23	55773	TBC1 domain family, member 23
TBR1	10716	T-box, brain 1
TC2N	123036	Tandem C2 domains, nuclear
TCEA2	6919	Transcription elongation factor A (SII), 2
TCN2	6948	Transcobalamin II; macrocytic anemia
TGOLN2	10618	Trans-golgi network protein 2
TIGD2	166815	Tigger transposable element derived 2

TIPIN	54962	TIMELESS interacting protein
TMEM11	8834	Transmembrane protein 11
TMEM37	140738	Transmembrane protein 37
TNRC18	84629	TNRC18
TOB1	10140	Transducer of ERBB2, 1
TOMM70A	9868	Translocase of outer mitochondrial membrane 70 homolog A (<i>S. cerevisiae</i>)
TP53I11	9537	Tumor protein p53 inducible protein 11
TSPAN7	7102	Tetraspanin 7
U2AF2	11338	U2 small nuclear RNA auxiliary factor 2
UBD	10537	Ubiquitin D
UQCR	10975	Ubiquinol-cytochrome c reductase, 6.4kDa subunit
USP12	219333	Ubiquitin specific peptidase 12
USP34	9736	Ubiquitin specific peptidase 34
UTRN	7402	Utrophin
WHSC2	7469	Wolf-Hirschhorn syndrome candidate 2
ZNF219	51222	Zinc finger protein 219
ZNF525	170958	Zinc finger protein 525
ZNF599	148103	Zinc finger protein 599
ZNF616	90317	Zinc finger protein 616
ZNRF1	84937	Zinc and ring finger 1

9.7. Abbreviations

ATM	ataxia telaniectasia mutated
bp	base pair
CDK	cyclin-dependent kinase
cDNA	complementary DNA
Ct	threshold cycle
CT	comparative threshold
DMSO	dimethyl sulfoxide
DNA	deoxyribonucleic acid
DNase	deoxyribonuclease
DSB	double stands break
dNTPs	deoxynucleotide triphosphates
EDTA	ethylene diamine tetraacetic acid
FBS	fetal bovine serum
FDR	false discovery rate
GAPDH	Glyseraldehyde-3-phosphate dehydrogenase
GLRX	Glutaredoxin
GO	The Gene Ontology Consortium
GSI	Gesellschaft für Schwerionenforschung
HEPES	4-(2-hydroxyethyl)-1-piperazineethanesulfonic acid
HI	heavy ion
IMT	Molecular Biology and Tumor Research, University Marburg
IPA	Ingenuity Pathway Analysis
LET	linear energy transfer
mRNA	messenger RNA
MRP	multidrug resistance-associated protein
NSCLC	non-small cell lung cancer
nt	nucleotide
OD	optical density
OSCC	oral squamous cell carcinoma
PBS	phosphate-buffered saline

PCR	polymerase chain reaction
qRT-PCR	quantitative RT-PCR
RBE	relative biological effectiveness
rpm	round per minute
RNA	ribonucleic acid
RNAase	ribonuclease
RT	room temperature
RT-PCR	real time PCR
SDS	sodium lauryl sulfate
SSC	saline-sodium citrate buffer
TAE	Tris-Acetate- EDTA buffer
Tris	Tris (hydroxymethyl) aminomethane
UV	ultraviolet radiation
MW	molecular weight

9.8. Curriculum Vitae

Family Name	You	First Name	An
Date of Birth	11.01.1982	Place of Birth	Wuhan, Hubei, China
Gender	Female	Nationality	China
Contacts			
Tel (Mobile)		0049-17635515633	
Address		Umgehungsstr.20f 35043 Marburg	
Email		You@student.uni-marburg.de	
Educations			
04. 2007-12. 2011	Student of Dr. med Department of Radiation Therapy and Radiooncology Philipps-University of Marburg, Germany Dissertation Project: Gene expression profiling of lung cancer cells irradiated by carbon ion and X-rays		
09. 2004-07. 2006	Master of Pharmaceutical Chemistry College of Pharmacy, Wuhan University Thesis: Application of High Performance Liquid Chromatography/Electrospray-Mass Spectrometry in the Determination of Several Drugs		
02. 2002-07. 2004	Bachelor of Life Science College of Life Science, Wuhan University		
09. 2000-07. 2004	Bachelor of Pharmacy College of Pharmacy, Wuhan University		
Professional Trainings			
04. 2007-11. 2011	Department of Radiation Therapy and Radiooncology Philipps-University of Marburg, Germany And GSI, Darmstadt, Germany Training in molecular biological technique related to heavy ion irradiation and X-ray		

09. 2005-10. 2005	Agilent Technologies, Beijing, China Training in operation of LC-MS
07. 2005-08. 2005	Agilent Technologies, Shanghai, China Training in operation of gas chromatography
09. 2003-06. 2004	College of Life Science, Wuhan University, China Training in molecular biological technique
10. 2002-02. 2003	College of Pharmacy, Wuhan University, China Training in pharmacological experiments and animal experiments

9.9. Publications

IF*

- Fokas E, You A (co-first author), Juricko J, Engenhardt-Cabillic R, An HX.: Genetic alterations after carbon ion irradiation in human lung adenocarcinoma cells. *Int J Oncol*. 2011 Jan;38(1):161-168. 2.571
- He HT, Fokas E, You A, Engenhardt-Cabillic R, An HX.: Siah1 proteins enhance radiosensitivity of human breast cancer cells. *BMC Cancer*. 2010 Aug 3;10:403. 2.485
- You A, Fokas E, Wang LF, He H, Kleb B, Niederacher D, Engenhardt-Cabillic R, An HX.: Expression of the Wnt antagonist DKK3 is frequently suppressed in sporadic epithelial ovarian cancer. *J Cancer Res Clin Oncol*. 2011 Apr;137(4):621-7. Epub 2010 Jun 9. 3.153
- Wang LF, Fokas E, Juricko J, You A, Rose F, Pagenstecher A, Engenhardt-Cabillic R, An HX.: Increased expression of EphA7 correlates with adverse outcome in primary and recurrent glioblastoma multiforme patients. *BMC Cancer*. 2008 Mar 25;8:79. 3.153
- Guo P, Li X, Wang J, You A.: Study on the compatibility of cefotaxime with tinidazole in glucose injection. *J Pharm Biomed Anal*. 2007 Apr 11;43(5):1849-1853. 2.733

*IF (Impact factor) were as reported in the 2010 *Journal Citation Report*[®] (Thomson Reuters 2011).

Posters/Abstracts

An HX, You A, Juricko, J, Fokas E, Hanze J, Rose F, Fournier C, Taucher-Scholz G, Engenhardt-Cabillic R.: Gene expression profiling of lung cancer cells irradiated by carbon and X-rays. 15th Degro 2009, *Strahlenther Onkol* 2009 185: 47-47.

An HX, Wang LF, You A, He HT, Fokas E, Engenhardt-Cabillic R.: Functional regulation of DNA demethylation by 53BP1 in DNA damage response. 17th Degro 2011, Wiesbaden.

9.10. Academic teachers

My academic teachers were Ms./ Mr. An, Arenz, Eilers, Engenhardt-Cabillic, Keusgen, Krause, Stiewe in University Marburg, and Ms. Fournier, Taucher-Scholz in GSI, Darmstadt.

9.11. Declaration

Ich erkläre ehrenwörtlich, dass ich die dem Fachbereich Pharmazie Marburg zur Promotionsprüfung eingereichte Arbeit mit dem Titel

Gene expression profiling of lung cancer cells irradiated by carbon ion and X-rays

am medizinischen Zentrum für Radiologie, der Klinik für Strahlentherapie und Radioonkologie, unter Leitung von Frau Prof. Dr. med. R. Engenhardt-Cabillic ohne sonstige Hilfe selbst durchgeführt und bei der Abfassung der Arbeit keine anderen als die in der Dissertation angeführten Hilfsmittel benutzt habe. Ich habe bisher weder an einem in- und ausländischem medizinischem Fachbereich ein Gesuch um Zulassung zur Promotion eingereicht noch die vorliegende Arbeit oder eine andere Arbeit als Dissertation vorgelegt.

Marburg, 22.10.2012

9.12. Acknowledgement

This dissertation required many help and support from many people, without their help, this complement of my dissertation could not be possible.

First of all, I would like to extend my sincere gratitude to my mentors, Prof. Dr. R. Engerhart-Cabillic and Prof. Dr. M. Keusgen, for their intellectual guidance, kindly understanding and professional instructions during my doctoral study, as well as, providing me with inspiring advices during the writing of my dissertation.

Technical support was of course crucial to all of my dissertation research. Grateful acknowledgments are made to Dr. Gisela Taucher-Scholz and Dr. Claudia Fournier GSI Darmstadt and Prof. Dr. Martin Eilers, Prof. Dr. Thorsten Stiewe and Dr. Michael Krause in IMT of University of Marburg, for all the convenience that they provided.

I owe a special debt of gratitude to Dr. Hanxiang An, for giving me endless academic support and meaningful feedback. I really appreciate for his great effort made to make my dissertation stronger and more insightful.

I would like to thank my beloved family for their loving considerations and great confidence in me all through these years.

Last, but not least, I would like to express my gratitude to all those who have helped me during my doctoral study, especially, to Mr. Fokas, Mrs. Kleb and Haitao He, for their kindly assistance and for the comfortable environment they provided in the lab.